



Contents lists available at ScienceDirect

Bioorganic & Medicinal Chemistry

journal homepage: www.elsevier.com/locate/bmc

Structure-based drug design of 1,3,5-triazine and pyrimidine derivatives as novel FGFR3 inhibitors with high selectivity over VEGFR2

Ikumi Kuriwaki^{a,*}, Minoru Kameda^a, Hiroyuki Hisamichi^{a,1}, Shigetoshi Kikuchi^{a,2}, Kazuhiko Iikubo^a, Yuichiro Kawamoto^{a,3}, Hiroyuki Moritomo^a, Yutaka Kondoh^{a,4}, Yasushi Amano^a, Yukihiro Tateishi^a, Yuka Echizen^a, Yoshinori Iwai^b, Atsushi Noda^b, Hiroshi Tomiyama^b, Tomoyuki Suzuki^a, Masaaki Hirano^a

^a Drug Discovery Research, Astellas Pharma Inc., 21 Miyukigaoka, Tsukuba, Ibaraki 305-8585, Japan

^b Research Laboratories, Kotobuki Pharmaceutical Co., Ltd., 198 Kamigomyou Sakaki-Machi, Hanishina-Gun, Nagano 389-0697, Japan

ARTICLE INFO

Keywords:

Fibroblast growth factor receptor 3
Vascular endothelial growth factor receptor 2
Kinase selectivity
Structure-based drug design
X-ray crystal structure
Structure activity relationships

ABSTRACT

Fibroblast growth factor receptor 3 (FGFR3) is an attractive therapeutic target for the treatment of bladder cancer. We identified 1,3,5-triazine derivative **18b** and pyrimidine derivative **40a** as novel structures with potent and highly selective FGFR3 inhibitory activity over vascular endothelial growth factor receptor 2 (VEGFR2) using a structure-based drug design (SBDD) approach. X-ray crystal structure analysis suggests that interactions between **18b** and amino acid residues located in the solvent region (Lys476 and Met488), and between **40a** and Met529 located in the back pocket of FGFR3 may underlie the potent FGFR3 inhibitory activity and high kinase selectivity over VEGFR2.

1. Introduction

Bladder cancer, a type of urothelial cancer, is the most common malignancy involving the urinary system and the ninth most common malignancy worldwide.¹ Bladder cancer is histologically classified into three major types: non-muscle invasive, muscle invasive and metastatic bladder cancer. Although the 5-year survival rate of non-muscle invasive bladder cancer (NMIBC) is over 70%, it recurs frequently or progresses to muscle invasive bladder cancer. Furthermore, the treatment outcome remains insufficient for muscle invasive and metastatic bladder cancers, with a 5-year survival rate of less than 50%.²

Current therapies for NMIBC are transurethral resection of the bladder tumor and intravesical postoperative Bacille de Calmette et Guérin (BCG) therapy or chemotherapy, which are insufficiently effective for relapse prevention.³ The main therapies for muscle invasive and metastatic bladder cancers are total bladder resection and systemic administration of chemotherapeutic agents, although these treatments are associated with low efficacy and side effects.³ Recently, immune checkpoint inhibitors, such as anti-PD-1 and anti-PD-L1 antibodies,

have been approved for the treatment of metastatic urothelial carcinoma. Although several complete response cases have been observed in clinical trials, their objective response rates were only 14–24%.⁴ Thus, more effective and safer molecularly targeted therapies for bladder cancer are warranted.

The signaling pathway activated by fibroblast growth factors (FGFs) and their receptors, fibroblast growth factor receptors (FGFRs), is one of the most important in the development from early embryogenesis to the formation of various organs.⁵ The mammalian FGF/FGFR family comprises 18 ligands and 4 main receptors (FGFR1, 2, 3, and 4). All FGFRs are single-transmembrane receptors and act as tyrosine kinases.⁵ FGFs induce FGFR dimerization, followed by FGFR autophosphorylation and activation of downstream signaling pathways such as PI₃K-AKT and Ras/Raf/MEK/MAPK.⁵ In a variety of human cancers, aberrant activation of FGF/FGFR signaling promotes cellular proliferation, migration/invasion and angiogenesis.⁵

Recent studies have reported that FGFR3 harbors activating gene mutations, mainly R248C, S249C, G372C, Y375C, and K652E, observed in about 50% of bladder cancer cases.^{6,7} Further, the FGFR gene and

* Corresponding author.

E-mail address: ikumi.kuriwaki@astellas.com (I. Kuriwaki).

¹ Present address: Industrial Property Cooperation Center, Fukagawa Gatharia W3 Building, 1-2-15 Kiba, Koto-ku, Tokyo 135-0042, Japan.

² Present address: Tsukuba Research Laboratories, Tokuyama Corporation, 40 Wadai, Tsukuba, Ibaraki 300-4247, Japan.

³ Present address: School of Life Sciences, Tokyo University of Pharmacy and Life Sciences, 1432-1 Horinouchi, Hachioji, Tokyo 192-0392, Japan.

⁴ Present address: Kishida Chemical Co., Ltd., 13-2 Ooaza-hoshinosato, Ami-machi, Inashiki-gun, Ibaraki 300-0326, Japan.

<https://doi.org/10.1016/j.bmc.2020.115453>

Received 9 February 2020; Received in revised form 18 March 2020; Accepted 20 March 2020

0968-0896/© 2020 Elsevier Ltd. All rights reserved.

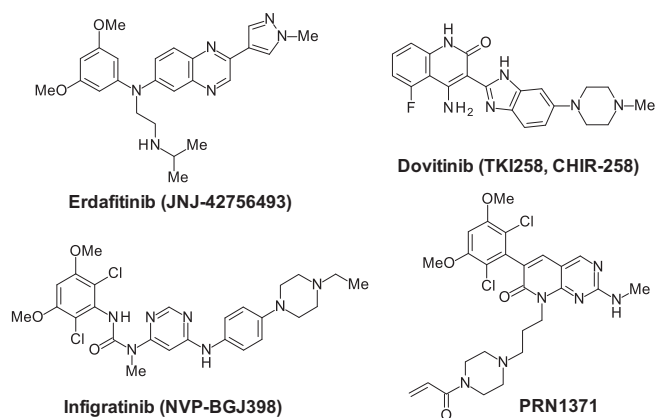


Fig. 1. Structure of erdafitinib (JNJ-42756493),¹² dovitinib (TKI258),¹⁸ infigratinib (NVP-BGJ398),²³ and PRN1371.²⁴

transforming acidic coiled-coil (TACC) fusion gene (FGFR3-TACC3 and FGFR3-BAIAP2L1) are reportedly expressed in a subset of bladder cancer patients.^{8,9,10} Therefore, clinical trials of FGFR3 inhibitors for bladder cancer patients harboring FGFR3 point mutations or fusion genes are currently being conducted.¹¹ The clinical relevance of FGFR3-targeted therapy has been suggested in reports on erdafitinib (JNJ-42756493; **Figure 1**),^{12,13} which has received accelerated approval from the U.S. Food and Drug Administration (FDA) for the treatment of adults with locally advanced or metastatic urothelial carcinoma in 2019.¹⁴ Given these findings, FGFR3 is considered an attractive target for novel therapies for bladder cancer.

In general, acquiring selective ATP-competitive kinase inhibitors is challenging due to the high conservation of amino acid residues in the kinase catalytic domain. Furthermore, low kinase selectivity tends to cause side effects. Interestingly, amino acid sequences in the catalytic domain of FGFR3 are similar to those of vascular endothelial growth factor receptor 2 (VEGFR2).¹⁵ Therefore, classical FGFR inhibitors have shown toxicity related to VEGFR2 inhibition.^{16,17} For example, dovitinib (TKI258, CHIR-258; **Fig. 1**), a clinical candidate FGFR inhibitor, inhibits both FGFR3 and VEGFR2 with IC₅₀ values of 9 nM and 13 nM, respectively (1-fold selectivity).^{18,19} In clinical trials, dovitinib causes hypertension as a side effect, which is attributed to its VEGFR2 inhibitory activity.^{20,21} Erdafitinib also shows inhibitory activity against both FGFR3 and VEGFR2 with IC₅₀ values of 3 nM and 36.8 nM, respectively (12-fold selectivity).²² Further, FGFR-selective inhibitors such as infigratinib (NVP-BGJ398) and RPN-1371 are currently undergoing clinical trials for the treatment of bladder cancer. These compounds show 180- and 172-fold higher selectivity for FGFR3 over VEGFR2 than erdafitinib, respectively.^{23,24}

Therefore, we hypothesized that potent FGFR3 inhibitors without VEGFR2 inhibitory activity would be promising drug candidates for the treatment of bladder cancer, and would not cause serious side effects such as hypertension. In this article, we describe the synthesis and structure-activity relationships (SARs) of 1,3,5-triazine and pyrimidine derivatives as potent and highly selective FGFR3 inhibitors.

2. Design and chemistry

2.1. Structure-based drug design (SBDD)

Compound **1**, which was identified as a FGFR3 inhibitor from our high throughput screening (HTS) library, exhibited moderate inhibitory activity against FGFR1, 2, and 3 with unsatisfactory selectivity over VEGFR2 (**Table 1**). To obtain kinase inhibitors that were highly selective over VEGFR2, we utilized X-ray crystal structure data to obtain insight on how to improve kinase selectivity.

To reveal the binding mode of **1**, we used the FGFR2 kinase domain

Table 1
In vitro activity of compound **1**.

Kinase	FGFR1	FGFR2	FGFR3	FGFR4	VEGFR2	Ratio ^a (fold)
IC ₅₀ (nM)	40	5.1	12	682	266	22

a: Ratio of IC₅₀ value of VEGFR2 to FGFR3.

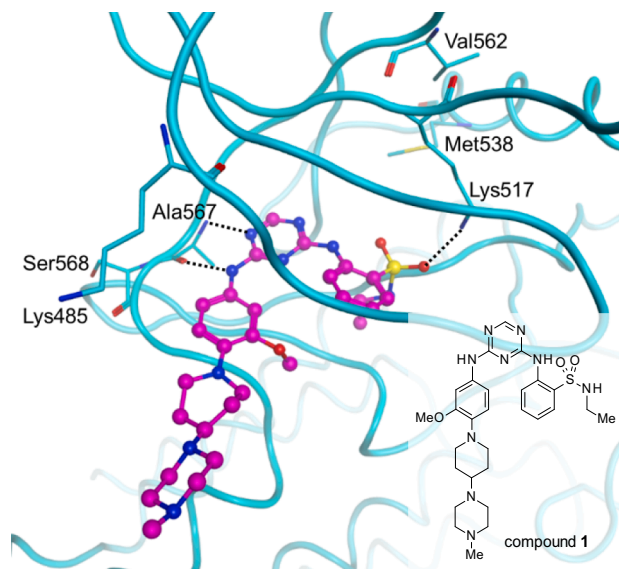


Fig. 2. X-ray crystal structure of **1** in complex with FGFR2 (PDB code: 6LVL).

as a surrogate. According to the X-ray crystal structure analysis of **1** in complex with FGFR2, **1** was located in the ATP binding site (**Fig. 2**). Among amino acid residues making up the ATP binding site, all residues were conserved between FGFR2 and FGFR3 except for Ser568 (corresponding to Ala559 in FGFR3), which was located outside the pocket. Therefore, we predicted the binding modes of compounds with FGFR3 based on the X-ray crystal structure using FGFR2. The 2-amino-1,3,5-triazine moiety formed hydrogen bonds with the main chain atoms of Ala567 (Ala558 in FGFR3) in the hinge region. In addition, the phenylsulfonamide moiety also formed a hydrogen bond with the side chain amino group of Lys517 (Lys508 in FGFR3). Based on the characteristic interactions with Ala567 and Lys517, we concluded that changing the 2-amino-1,3,5-triazine and phenylsulfonamide moieties would not lead to optimization of the structure of **1**. In contrast, the 3-methoxy-4-[4-(4-methylpiperazin-1-yl)piperidin-1-yl]phenyl moiety was exposed to the solvent region and formed no interactions. Among the amino acid residues located adjacent to the solvent region, the side chain amino group of Lys485 (Lys476 in FGFR3) could act as a hydrogen bond donor. Thus, a compound that can interact with Lys476 is expected to exhibit high inhibitory activity against FGFR3. Further, **1** did not interact with the hydrophobic residues in the back pocket, such as Met538 (Met529 in FGFR3) and Val562 (Val553 in FGFR3). In particular, Met529 in FGFR3 is not conserved in VEGFR2 (corresponding to Leu889), suggesting that achievement of an interaction with Met529 may enhance the inhibitory activity of FGFR3 and improve selectivity over VEGFR2.

We planned two synthetic strategies based on the X-ray crystal structure analysis findings described above. First, to acquire an

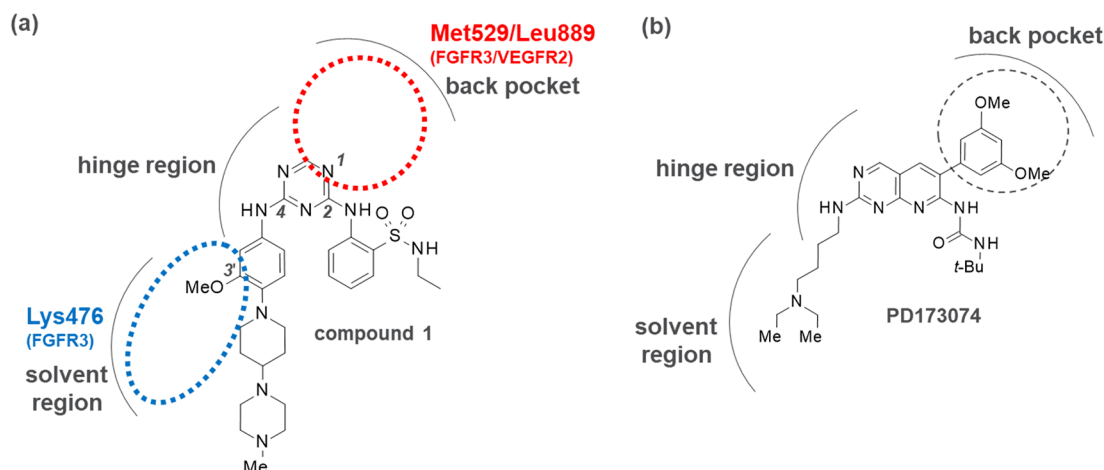


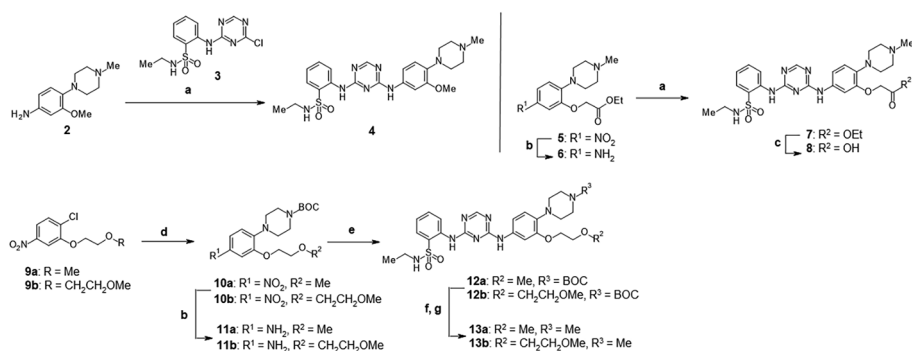
Fig. 3. (a) Illustration of representative kinase pockets and targeted amino acid residues with compound 1. (b) Structure of PD173074 with the representative kinase pockets.²⁵

interaction via a hydrogen bond with the Lys476 adjacent to the solvent region, we introduced a hydrogen bond acceptor into the 3'-position of the benzene ring at the right side of 1 (blue circle in Fig. 3a). We expect that the 3'-methoxy moiety can easily rotate to the opposite side of the benzene ring due to sufficient space around the 3'-position. Therefore, we designed compounds based on further extension of the methoxy moiety. Optimization of a linker was also important for adjusting the distance from the 3'-position to the side chain of Lys476. Second, to achieve a hydrophobic interaction with Met529 in the back pocket, we identified the 1-position of 1,3,5-triazine as the most favorable site for accessing the back pocket. Although the 1-position of 1,3,5-triazine cannot be substituted, the 1,3,5-triazine scaffold can be replaced with a pyrimidine because the nitrogen atom at the 1-position did not show any interactions in the X-ray structural analysis (red circle in Fig. 3a).

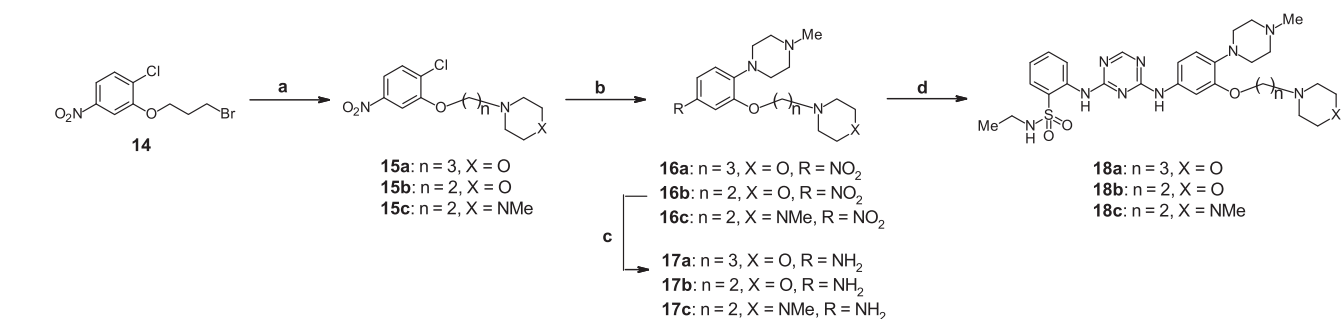
To fill the back pocket, we introduced a 3,5-dimethoxyphenyl group, a substructure of PD173074 (Fig. 3b), to the corresponding position of the pyrimidine.²⁵ PD173074 is a known classical FGFR inhibitor and is capable of filling the back pocket according to X-ray structural analysis.²⁵ In addition, careful optimization of a linker was also necessary to identify steric differences between the side chain of Met529 in FGFR3 and Leu889 in VEGFR2.

2.2. Chemistry

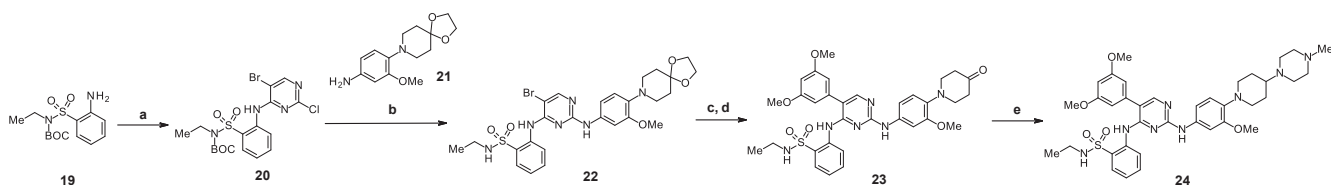
Synthesis of the target compounds is outlined in Schemes 1–6. The synthesis of compounds 4, 7, 8, 13a, and 13b is shown in Scheme 1. Commercially available 2 was reacted with 3²⁶ to give 4 via a nucleophilic aromatic substitution (S_NAr) reaction under acidic condi-



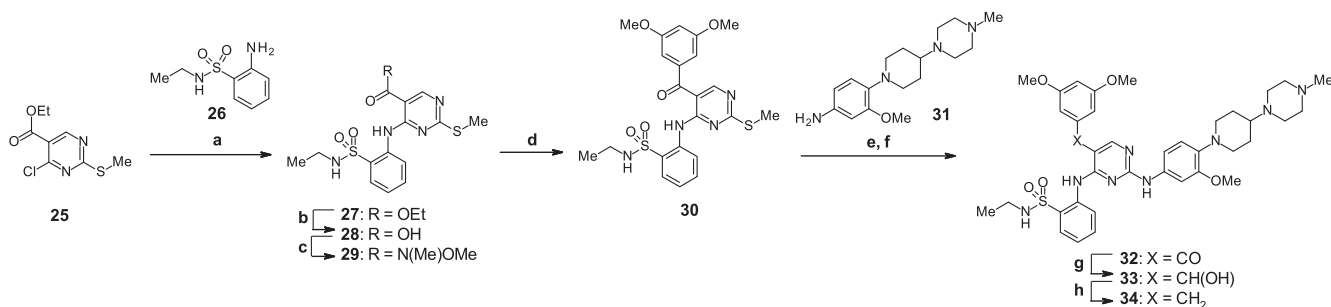
Scheme 1. Reagents and conditions: (a) 3, methanesulfonic acid, EtOH, 80 °C or 100 °C; (b) H₂, Pd/C, MeOH, room temperature; (c) 10% NaOH aq., EtOH, 80 °C; (d) 1-(*tert*-butoxycarbonyl)piperazine, K₂CO₃, DMF, 80 °C; (e) 3, DIPEA, NMP, microwave (μ W), 120 °C; (f) TFA, CH₂Cl₂, room temperature; (g) 37% HCHO aq., NaBH(OAc)₃, CH₂Cl₂, room temperature.



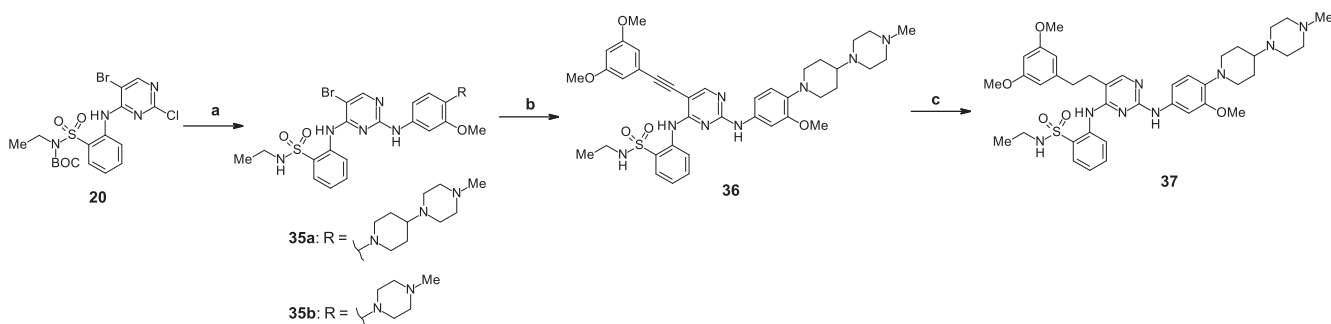
Scheme 2. Reagents and conditions: (a) morpholine, K₂CO₃, KI, MeCN, 60 °C; (b) *N*-methyl-piperazine, K₂CO₃, NMP or DMSO, 150 °C; (c) FeCl₃ hexahydrate, hydrazine monohydrate, activated carbon, EtOH/H₂O, 80 °C or 100 °C; (d) 3, AcOH, room temperature.



Scheme 3. Reagents and conditions: (a) 5-bromo-2,4-dichloropyrimidine, NaH, THF, 50 °C; (b) **21**, DIPEA, NMP/IPA, μ W, 150 °C; (c) 3,5-dimethoxyphenylboronic acid, Pd(PPh₃)₄, Na₂CO₃, 1,4-dioxane/H₂O, 110 °C; (d) AcOH/H₂O, 100 °C; (e) *N*-methyl-piperazine, NaBH(OAc)₃, Et₃N, CH₂Cl₂, room temperature.



Scheme 4. Reagents and conditions: (a) **26**, DIPEA, NMP, 130 °C; (b) 1 M NaOH aq., THF/MeOH, room temperature; (c) *N,O*-dimethylhydroxylamine hydrochloride, EDCI hydrochloride, HOBT, Et₃N, DMF, room temperature; (d) 3,5-dimethoxyphenylmagnesium bromide, THF, -78 °C to room temperature; (e) *m*-CPBA, CH₂Cl₂, room temperature; (f) **31**, IPA, 90 °C; (g) NaBH₄, THF/MeOH, room temperature; (h) triethylsilane, TFA, CH₂Cl₂, room temperature.

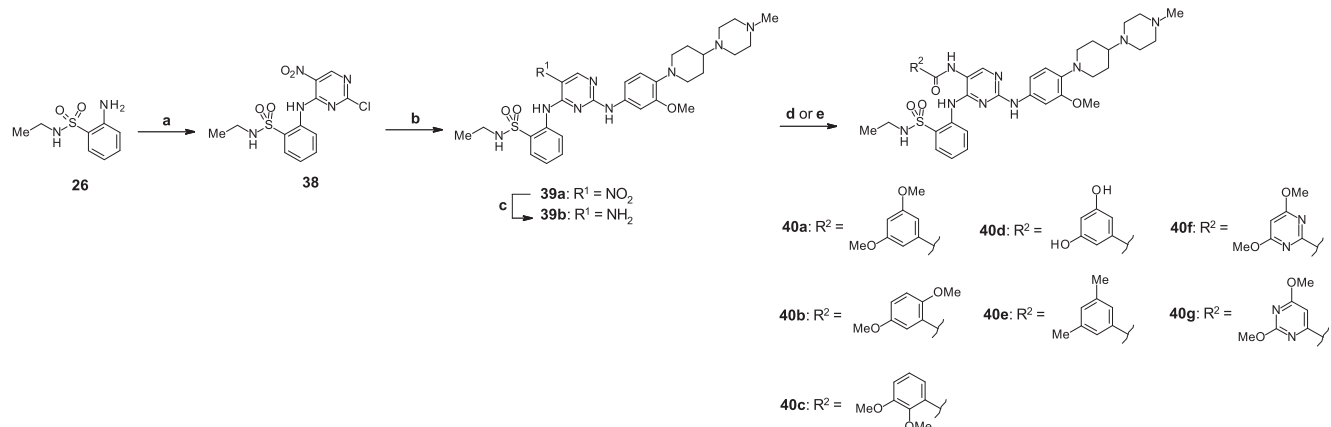


Scheme 5. Reagents and conditions: (a) **31** or **2**, methanesulfonic acid, IPA, μ W, 130 °C; (b) 1-ethynyl-3,5-dimethoxybenzene, Pd(PPh₃)₄, CuI, Et₃N, DMF, 120 °C; (c) H₂, Pd/C, MeOH/THF, room temperature.

tions. Reduction of nitro compound **5**²⁷ gave **6**, which was converted to **7** by an S_NAr reaction with **3**. Hydrolysis of ester **7** led to **8**. Introduction of a 1-(*tert*-butoxycarbonyl)piperazine unit to commercially available **9a** and **9b** gave **10a** and **10b**, which were subsequently transformed to **11a** and **11b** via hydrogenation of the nitro moiety. S_NAr

reaction of **11a** and **11b** with **3** gave **12a** and **12b**, which were converted to **13a** and **13b** by deprotection of the *tert*-butoxycarbonyl (BOC) moiety and subsequent methylation.

Scheme 2 shows the synthesis of compounds **18a–c**. Compound **15a** was prepared by alkylation of commercially available **14** with



Scheme 6. Reagents and conditions: (a) 2,4-dichloro-5-nitropyrimidine, DMAc, room temperature; (b) **31**, AcOH, room temperature; (c) H₂, Pd/C, EtOH/THF, room temperature; (d) 3,5-dimethoxybenzoyl chloride, DIPEA, THF, room temperature; (e) aryl carboxylic acid, HATU, DIPEA, DMF, room temperature.

morpholine. Subsequent introduction of the *N*-methyl-piperazine unit to **15a** or commercially available **15b** and **15c** yielded **16a–c**, which was followed by reduction of the nitro moiety using hydrazine monohydrate to give **17a–c**. Corresponding aryl amines **17a–c** were substituted with **3** to give **18a–c** via an S_NAr reaction.

Compound **24** was synthesized according to Scheme 3. Aryl amine **19**²⁸ was reacted with 5-bromo-2,4-dichloropyrimidine to give **20**, which was subsequently converted to **22** by introduction of **21**.²⁹ Suzuki coupling reaction of **22** with 3,5-dimethoxyphenylboronic acid gave the intermediate, and subsequent hydrolysis of the ketal group gave **23**. Compound **24** was obtained by reductive amination of **23** with *N*-methyl-piperazine.

The synthesis of compound **34** is shown in Scheme 4. S_NAr reaction between commercially available **25** and **26** gave **27**, which was subsequently converted to **28** by hydrolysis of the ester group. The carboxylic acid moiety of **28** was transformed to a phenyl ketone using Grignard reagent via Weinreb amide **29**.³⁰ The sulfide group of **30** was oxidized using *m*-CPBA to give sulfoxide, which was substituted with commercially available **31** to yield **32**. Reduction of the ketone moiety of **32** using $NaBH_4$ gave **33**, which was converted to **34** by deoxygenation with triethylsilane.

Scheme 5 shows the synthesis of compounds **35b** and **37**. Compound **20** was introduced to **31** or **2** via an S_NAr reaction to give **35a** and **35b**. Compound **35a** was coupled with 1-ethynyl-3,5-dimethoxybenzene by a Sonogashira reaction to give **36**. The alkyne linkage of **36** was reduced to yield **37**.

Compounds **40a–g** were synthesized according to Scheme 6. Compound **26** was reacted with 2,4-dichloro-5-nitropyrimidine by an S_NAr reaction to give **38**, which was subsequently converted to **39a** by introduction of **31** under acidic condition. Reduction of the nitro group of **39a** gave **39b**, which was treated with 3,5-dimethoxybenzoyl chloride or condensed with the corresponding aryl carboxylic acid to yield **40a–g**.

3. Results and discussion

The synthesized compounds were evaluated using an ADP-Glo luminescent kinase assay with human recombinant FGFR3 and VEGFR2 enzymes.

3.1. Results of targeting the interaction with Lys476 located adjacent to the solvent region

Table 2 shows the FGFR3 and VEGFR2 inhibitory activities of 1,3,5-triazine derivatives. Although the amine moiety at the 4'-position of **4** was different from that of **1**, it showed the same tendency for both potency and selectivity (based on the results for **1** and **4**). Therefore, the *N*-methyl-piperazine unit was substituted in every evaluated compound in this table. Introduction of various C2 units, such as an ester (**7**), carboxylic acid (**8**), and ether (**13a**), did not result in any enhancement of FGFR3 inhibitory activity compared to that of **4**. Next, we evaluated compounds with longer linker groups attached to a linear or cyclic ether moiety. Although **13b** did not show improved FGFR3 inhibitory activity, **18b** showed highly potent and specific FGFR3 inhibitory activity with IC_{50} values of 4.1 nM (FGFR3) and 570 nM (VEGFR2), respectively (139-fold selectivity). Interestingly, introduction of an *N*-methyl-piperazine moiety (**18c**) instead of morpholine (**18b**), and propylene linker (**18a**) instead of ethylene decreased FGFR3 inhibitory activity.

3.2. Discussion of the adapted strategy based on structural information on 18b

To confirm whether **18b** would undergo the expected interactions, we performed X-ray structural analysis. FGFR2 was again used as a surrogate. Similar to **1**, compound **18b** formed hydrogen bonds with Ala567 and Lys517 in FGFR2, according to the crystal structure of the

complex between FGFR2 and **18b** (Fig. 4). As expected, the oxygen atom of the morpholine moiety of **18b** formed a weak hydrogen bond (3.1 Å) with the side chain amino group of Lys485 in FGFR2. Therefore, the C2 linkers such as **7**, **8**, and **13a** were thought to be too short to reach the side chain amino group of Lys476. In addition, the results of **18a–c** suggested that the presence and location of an oxygen atom were important for the interaction with Lys485.

Unexpectedly, the methylene unit of the morpholine moiety of **18b** formed a hydrophobic interaction with the side chain of Met497 in FGFR2 (Met488 in FGFR3), which corresponds to Glu848 in VEGFR2. In the case of VEGFR2, such a hydrophobic interaction with the side chain of Glu848 might be weaker because Glu848 is a hydrophilic amino acid. These interactions with Lys485 and Met497 in FGFR2 by the morpholine moiety of **18b** are expected to contribute to the potent inhibitory activity against FGFR3 and improved selectivity over VEGFR2.

3.3. Results of targeting the interaction with Met529 in the back pocket

Table 3 shows the FGFR3 and VEGFR2 inhibitory activities of the pyrimidine derivatives. Direct introduction of a 3,5-dimethoxyphenyl ring to the 5-position of pyrimidine **24** increased the FGFR3 inhibitory activity, with an IC_{50} value of 4.1 nM (ca. 3-fold more potent than **1**). However, the kinase selectivity of **24** did not improve. Next, we evaluated compounds with a linker between the 5-position of pyrimidine and 3,5-dimethoxybenzene. Introduction of a methylene linker (**34**) resulted in a reduction in FGFR3 inhibitory activity, whereas an ethylene linker (**37**) retained potency. In addition, **37** showed improved selectivity over VEGFR2, with a decrease in VEGFR2 inhibitory activity at an IC_{50} value of 292 nM (ca. 8-fold less potent than **24**). Furthermore, replacement of ethylene with an amide linker (**40a**) resulted in a significant reduction in VEGFR2 inhibitory activity (>233-fold selectivity).

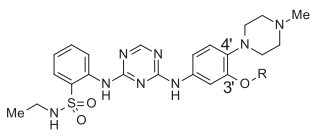
Finally, we examined the effect of substituting the phenyl moiety. Conversion of the 3,5-dimethoxyphenyl moiety, such as shifting the position of the dimethoxy moiety (**40b** and **40c**) and replacing it with other substituents (**40d** and **40e**), resulted in a reduction in FGFR3 inhibitory activity compared to **40a**. In contrast, introduction of pyrimidine instead of benzene enhanced VEGFR2 inhibitory activity (**40f** and **40g**) compared to **40a**. The 3,5-dimethoxyphenyl moiety was the best substituent for obtaining both potency and selectivity among these compounds.

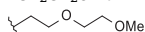
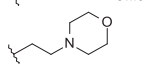
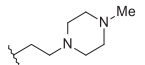
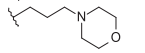
3.4. Discussion of the adopted strategy based on structural information on 37

The X-ray structure of **37** with FGFR3 is shown in Fig. 5a. Similar to **1** and **18b**, compound **37** formed hydrogen bonds with Ala558 and Lys508 in FGFR3. As expected, the 3,5-dimethoxyphenyl moiety occupied the back pocket and formed hydrophobic interactions. Specifically, this substituent formed van der Waals (vdW) interactions. We predicted that **24** did not improve the selectivity over VEGFR2 because, while the 3,5-dimethoxybenzene of **24** located in the back pocket, it was unable to reach the side chain of Met529 in FGFR3. Further, compound **35b** (5-bromopyrimidine derivative, structure shown in Scheme 5) also exhibited low kinase selectivity with IC_{50} values of 1.8 nM (FGFR3) and 6.6 nM (VEGFR2). In addition, studies have reported that a 5-bromopyrimidine scaffold like that of **35b** often shows multi-kinase inhibition.^{31,32} Our results suggested that the 3,5-dimethoxybenzene of **24** had a similar effect to that of a bromide moiety.

Fig. 5b shows the detailed structure of the back pocket in comparison with VEGFR2 (PDB code 4AG8).³¹ The 3,5-dimethoxyphenyl moiety of **37** formed vdW interactions with the S δ and C ϵ atoms of Met529 in FGFR3. In contrast, this substituent formed vdW interactions with only the C δ atom of Leu889 in VEGFR2. These interactions in the back pocket, especially with Met529, are thought to be responsible for maintaining the inhibitory activity against FGFR3 and improving the

Table 2
SARs of 1,3,5-triazine derivatives.



Compound	R	Enzyme IC ₅₀ (nM)		Ratio ^a (fold)
		FGFR3	VEGFR2	
4	-Me	15	341	23
7	-CH ₂ CO ₂ Et	62	316	5
8	-CH ₂ CO ₂ H	65	120	2
13a	-CH ₂ CH ₂ OMe	17	310	18
13b		21	550	26
18b		4.1	570	139
18c ^b		15	341	23
18a		63	736	12

a: Ratio of IC₅₀ value of VEGFR2 to FGFR3.

b: Tetrahydrochloride salt.

selectivity over VEGFR2. The kinase selectivity of **40a** was greater than that of **37**, suggesting that the amide linker was more rigid and slightly shorter than the ethylene linker. Such differences were thought to restrict **40a** from being positioned close to the side chain of Leu889 and weaken the interaction between the 3,5-dimethoxyphenyl moiety and Leu889, and contribute to the high selectivity of **40a** over VEGFR2. Subsequently, **40f** and **40g** showed potent VEGFR2 inhibitory activity compared to **40a** possibly because the two nitrogen atoms enhanced the vdW interaction between the dimethoxy moiety and Leu889.

3.5. Further pharmacological evaluations of **40a**

Given the promising features of **40a** including potent FGFR3 inhibitory activity and selectivity over VEGFR2, we further examined this compound in a pharmacological study. Compound **40a** showed pan-FGFR inhibitory activity with IC₅₀ values of 2.1 nM (FGFR1), 3.1 nM (FGFR2), and 74 nM (FGFR4). In addition, this compound suppressed proliferation of a UM-UC-14 human bladder cancer cell line, which expresses a FGFR3 S249C point mutation, with an IC₅₀ value of 84 nM.

4. Conclusion

We conducted structural optimization of compound **1**, identified in a HTS, to explore novel FGFR3 inhibitors with decreased activity against VEGFR2 via an SBDD approach. Following X-ray crystal structure analysis, we performed studies based on the Lys476 in the solvent region and Met529 in the back pocket of FGFR3. Structural optimization led to identification of 1,3,5-triazine derivative **18b** and pyrimidine derivative **40a**, which showed potent FGFR3 inhibitory activity with high selectivity over VEGFR2. In particular, **40a** is more attractive lead compound because of the significant reduction in VEGFR2 inhibitory activity. Further optimization studies of **40a** will be reported in due course.

5. Experimental

5.1. Chemistry

¹H-NMR spectra were recorded on Varian 400, Varian VNS-400,

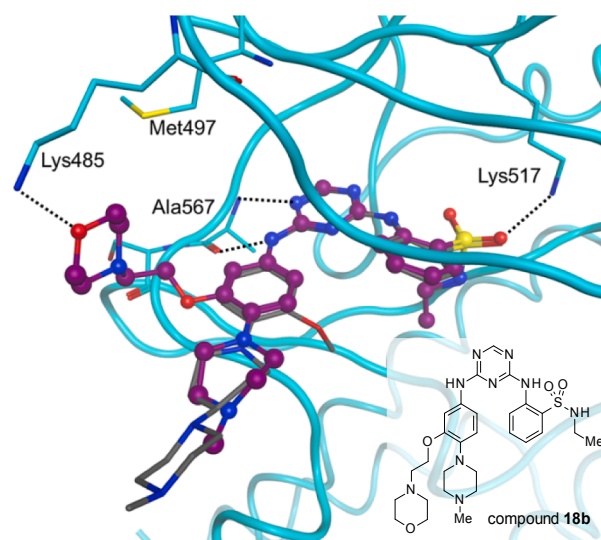


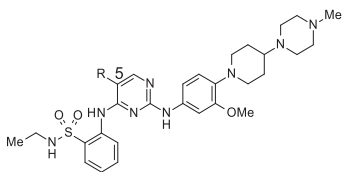
Fig. 4. X-ray crystal structure of **18b** in complex with FGFR2 (PDB code: 6LVK). **1** is superimposed and shown as a gray stick model in gray.

Varian 400-MR, JEOL Lambda, or JEOL EX-400, and chemical shifts are expressed in δ (ppm) values with tetramethylsilane as an internal reference (s = singlet, d = doublet, t = triplet, q = quartet, m = multiplet, dd = doublet of doublets, qd = quartet of doublets, and br = broad peak). Mass spectra (MS) were recorded on Thermo Electron LCQ Advantage, Thermo Electron TSQ 700, Waters ZQ2000, Waters SQD, or Agilent Quadrupole. Electrospray ionization (ESI) positive high resolution mass spectra (HRMS) were obtained using Thermo Fisher EXACTIVE-Plus. Elemental analyses were performed with Yanaco MT-6 (C, H, N), Elementar Vario MICRO cube (C, H, N), Elementar Vario EL (C, H, N), DIONEX DX-500 (S, halogen), DIONEX ICS-2000 (S, halogen), or DIONEX ICS-3000 (S, halogen) instruments, and the results were within $\pm 0.3\%$ of theoretical values. The following abbreviations are used: AcOH, acetic acid; MeCN, acetonitrile; HATU, O-(7-aza-1H-benzotriazol-1-yl)-N,N,N',N'-tetramethyluronium hexafluorophosphate; *m*-CPBA, 3-chloroperoxybenzoic acid; Et₂O, diethyl ether; IPE, diisopropyl ether; DIPEA, *N,N*-diisopropylethylamine; DMSO, dimethyl sulfoxide; DMAC, *N,N*-dimethylacetamide; DMF, *N,N*-dimethylformamide; EtOH, ethanol; EtOAc, ethyl acetate; EDCl, 1-ethyl-3-(3-dimethylaminopropyl)carbodiimide; HOBt, 1-hydroxybenzotriazole monohydrate; IPA, isopropyl alcohol; MeOH, methanol; NMP, 1-methyl-2-pyrrolidone; NaBH(OAc)₃, sodium triacetoxyborohydride; THF, tetrahydrofuran; Et₃N, triethylamine; TFA, trifluoroacetic acid; PPh₃, triphenylphosphine.

5.1.1. *N*-Ethyl-2-((4-[3-methoxy-4-(4-methylpiperazin-1-yl)anilino]-1,3,5-triazin-2-yl)amino)benzene-1-sulfonamide (**4**)

To a solution of 3-methoxy-4-(4-methylpiperazin-1-yl)aniline (**2**, 120 mg, 0.54 mmol) in EtOH (3.0 mL) was added methanesulfonic acid (70 μ L, 1.08 mmol). The mixture was stirred at room temperature for 15 min, and 2-[(4-chloro-1,3,5-triazin-2-yl)amino]-*N*-ethylbenzene-1-sulfonamide (**3**, 204 mg, 0.65 mmol) was added. After stirring at 80 °C for 2 h, the mixture was neutralized with sat. NaHCO₃ aq. and then extracted with EtOAc. The organic layer was washed with brine dried over MgSO₄ and concentrated *in vacuo*. The residue was purified by column chromatography on silica gel (CHCl₃/MeOH/28% NH₃ aq. = 100:0:0 to 100:10:1) to give the product (102 mg, 38%) as a beige solid. ¹H NMR (CDCl₃): δ 1.04 (3H, t, *J* = 7.3 Hz), 2.37 (3H, s), 2.54–2.73 (4H, m), 2.99 (2H, q, *J* = 7.3 Hz), 3.03–3.17 (4H, m), 3.84 (3H, br s), 4.79–4.99 (1H, m), 6.85–6.93 (1H, m), 6.93–7.01 (1H, m), 7.15–7.23 (1H, m), 7.28–7.43 (1H, m), 7.49–7.63 (1H, m), 7.93 (1H, dd, *J* = 7.8, 1.5 Hz), 8.37 (1H, br s), 8.45 (1H, d, *J* = 7.8 Hz), 8.74–9.07 (1H, m); MS (ESI) *m/z* [M+H]⁺ 499; Anal. Calcd for

Table 3
SARs of pyrimidine derivatives.



Compound	R	Enzyme IC ₅₀ (nM)		Ratio ^a (fold)
		FGFR3	VEGFR2	
24		4.1	38	9
34		> 1000	> 1000	NC ^b
37		2.8	292	104
40a		4.3	> 1000	> 233
40b		54	435	8
40c		40	461	12
40d		35	715	20
40e		275	554	2
40f		1.8	131	73
40g		34	227	7

a: Ratio of IC₅₀ value of VEGFR2 to FGFR3.

b: Not calculated.

C₂₃H₃₀N₈O₃S·0.3CHCl₃·0.6H₂O: C, 51.33; H, 5.82; N, 20.55; S, 5.88; Cl, 5.85. Found: C, 51.37; H, 5.73; N, 20.51; S, 5.82; Cl, 5.62.

5.1.2. Ethyl [5-amino-2-(4-methylpiperazin-1-yl)phenoxy]acetate (**6**)

To a solution of ethyl [2-(4-methylpiperazin-1-yl)-5-nitrophenoxy]acetate (**5**, 275 mg, 0.85 mmol) in MeOH (3 mL) was added 5% Pd/C (50% wet, 30 mg) under an argon atmosphere. After stirring at room temperature under a hydrogen atmosphere for 7 h, the mixture was passed through a Celite pad and washed with MeOH. The filtrate was concentrated *in vacuo*. The residue was purified by column chromatography on silica gel (CHCl₃/MeOH = 25:1 to 10:1) to give the product (180 mg, 72%) as a brown oil. ¹H NMR (CD₃OD): δ 1.29 (3H, t, *J* = 7.2 Hz), 2.66 (3H, s), 2.92–3.30 (8H, m), 4.24 (2H, q, *J* = 7.2 Hz), 4.68 (2H, s), 6.32–6.34 (2H, m), 6.80 (1H, d, *J* = 9.2 Hz); MS (ESI) *m/z* [M + H]⁺ 294.

5.1.3. Ethyl [5-({4-[2-(ethylsulfamoyl)anilino]-1,3,5-triazin-2-yl}amino)-2-(4-methylpiperazin-1-yl)phenoxy]acetate (**7**)

To a solution of **6** (180 mg, 0.61 mmol) in EtOH (4 mL) was added methanesulfonic acid (66 μL, 1.02 mmol). The mixture was stirred at room temperature for 20 min, and **3** (160 mg, 0.51 mmol) was added.

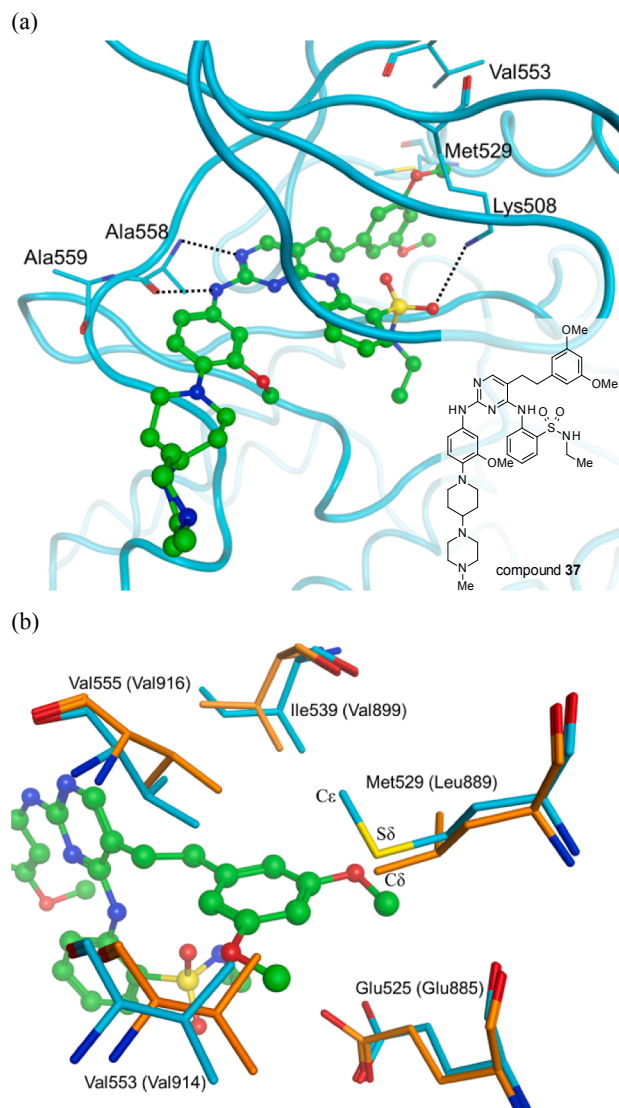


Fig. 5. (a) X-ray crystal structure of **37** in complex with FGFR3 (PDB code: 6LVM). (b) The same as (a) with focus on the back pocket. Superimposed structure of FGFR3 and VEGFR2 (PDB code: 4AG8).³³ Amino acid residues making up the back pocket are shown using a cyan and orange stick model for FGFR3 and VEGFR2, respectively. Residue names of VEGFR2 are shown in parentheses.

After stirring at 100 °C for 3 h, the mixture was neutralized with sat. NaHCO₃ aq. and extracted with EtOAc. The organic layer was washed with brine, dried over Na₂SO₄ and concentrated *in vacuo*. The residue was purified by column chromatography on silica gel (CHCl₃/MeOH = 50:1 to 20:1) to give the product (141 mg, 49%) as a yellow solid. ¹H NMR (CDCl₃): δ 1.05 (3H, t, *J* = 7.2 Hz), 1.28 (3H, t, *J* = 7.2 Hz), 2.37 (3H, s), 2.50–2.75 (4H, m), 2.98 (2H, q, *J* = 7.2 Hz), 3.01–3.28 (4H, m), 4.26 (2H, q, *J* = 7.2 Hz), 4.66 (2H, br s), 5.54 (1H, br s), 6.88–6.95 (2H, m), 7.17–7.21 (1H, m), 7.26–7.72 (3H, m), 7.94 (1H, dd, *J* = 8.0, 1.6 Hz), 8.33 (1H, br s), 8.42 (1H, d, *J* = 8.4 Hz), 8.92 (1H, br s); HRMS (ESI) *m/z* Calcd for C₂₆H₃₅N₈O₅S [M + H]⁺: 571.2446. Found: 571.2444.

5.1.4. [5-({4-[2-(ethylsulfamoyl)anilino]-1,3,5-triazin-2-yl}amino)-2-(4-methylpiperazin-1-yl)phenoxy]acetic acid (**8**)

To a solution of **7** (116 mg, 0.20 mmol) in EtOH (1 mL) was added 10% NaOH aq. (0.3 mL). After stirring at 80 °C for 1 h, the mixture was concentrated *in vacuo*. The residue was diluted with H₂O, and 10% HCl aq. was added to the mixture. The resulting precipitate was filtered and

dried to give the product (46 mg, 42%) as a pale yellow solid. $^1\text{H NMR}$ (CD_3OD): δ 1.00 (3H, t, $J = 7.2$ Hz), 2.89–3.33 (9H, m), 3.51–3.76 (4H, m), 4.60 (2H, br s), 6.97 (1H, d, $J = 8.8$ Hz), 7.17–7.25 (2H, m), 7.35–7.45 (1H, m), 7.51–7.63 (1H, m), 7.90 (1H, dd, $J = 8.0$, 1.6 Hz), 8.33–8.54 (2H, m); HRMS (ESI) m/z Calcd for $\text{C}_{24}\text{H}_{31}\text{N}_8\text{O}_5\text{S}$ $[\text{M} + \text{H}]^+$: 543.2133. Found: 543.2138.

5.1.5. *tert*-Butyl 4-[2-(2-methoxyethoxy)-4-nitrophenyl]piperazine-1-carboxylate (**10a**)

To a solution of 1-chloro-2-(2-methoxyethoxy)-4-nitrobenzene (**9a**, 4.229 g, 18.26 mmol) in DMF (40 mL) were added 1-(*tert*-butoxycarbonyl)piperazine (3.400 g, 18.26 mmol) and K_2CO_3 (5.047 g, 36.52 mmol). After stirring at 80 °C for 48 h, the mixture was diluted with H_2O and extracted with EtOAc. The organic layer was washed with H_2O followed by brine, dried over Na_2SO_4 and concentrated *in vacuo*. The residue was purified by column chromatography on silica gel (*n*-hexane/EtOAc = 9:1 to 5:1) to give the product (1.560 g, 22%) as a yellow oil. $^1\text{H NMR}$ (CDCl_3): δ 1.49 (9H, s), 3.15–3.25 (4H, m), 3.45 (3H, s), 3.54–3.64 (4H, m), 3.79–3.81 (2H, m), 4.21–4.23 (2H, m), 6.85 (1H, d, $J = 8.8$ Hz), 7.71 (1H, d, $J = 2.4$ Hz), 7.86 (1H, dd, $J = 8.8$, 2.8 Hz); MS (ESI) m/z $[\text{M} + \text{H}]^+$ 382.

5.1.6. *tert*-Butyl 4-{2-[2-(2-methoxyethoxy)ethoxy]-4-nitrophenyl}piperazine-1-carboxylate (**10b**)

Compound **10b** was prepared from 1-chloro-2-[2-(2-methoxyethoxy)ethoxy]-4-nitrobenzene (**9b**) in 15% yield using a similar approach to that described for **10a**. $^1\text{H NMR}$ (CDCl_3): δ 1.49 (9H, s), 3.14–3.28 (4H, m), 3.38 (3H, s), 3.55–3.61 (6H, m), 3.69–3.71 (2H, m), 3.89–3.91 (2H, m), 4.23–4.26 (2H, m), 6.85 (1H, d, $J = 8.8$ Hz), 7.71 (1H, d, $J = 2.8$ Hz), 7.85 (1H, dd, $J = 8.8$, 2.4 Hz); MS (ESI) m/z $[\text{M} + \text{H}]^+$ 426.

5.1.7. *tert*-Butyl 4-[4-amino-2-(2-methoxyethoxy)phenyl]piperazine-1-carboxylate (**11a**)

Compound **11a** was prepared from **10a** in 98% yield using a similar approach to that described for **6**. $^1\text{H NMR}$ (CDCl_3): δ 1.48 (9H, s), 3.41 (3H, s), 3.53–3.76 (6H, m), 3.94–4.10 (4H, m), 4.14–4.17 (2H, m), 6.28–6.31 (2H, m), 7.94–8.11 (1H, m); MS (ESI) m/z $[\text{M} + \text{H}]^+$ 352.

5.1.8. *tert*-Butyl 4-{4-amino-2-[2-(2-methoxyethoxy)ethoxy]phenyl}piperazine-1-carboxylate (**11b**)

Compound **11b** was prepared from **10b** in 74% yield using a similar approach to that described for **6**. $^1\text{H NMR}$ (CDCl_3): δ 1.48 (9H, s), 3.36 (3H, s), 3.36–3.80 (8H, m), 3.84–3.86 (2H, m), 3.98–4.15 (4H, m), 4.18–4.21 (2H, m), 6.32–6.34 (2H, m), 7.98–8.21 (1H, m); MS (ESI) m/z $[\text{M} + \text{H}]^+$ 396.

5.1.9. *tert*-Butyl 4-[4-{4-[2-(ethylsulfamoyl)anilino]-1,3,5-triazin-2-yl}amino]-2-(2-methoxyethoxy)phenyl]piperazine-1-carboxylate (**12a**)

To a solution of **11a** (187 mg, 0.53 mmol) and **3** (200 mg, 0.64 mmol) in NMP (2 mL) was added DIPEA (180 μL , 1.06 mmol). After stirring at 120 °C under microwave irradiation for 20 min, the mixture was diluted with H_2O . The resulting precipitate was filtered and dried. The obtained solid was purified by column chromatography on silica gel (*n*-hexane/EtOAc = 2:1 to 1:2) to give the product (120 mg, 36%) as a brown solid. $^1\text{H NMR}$ (CDCl_3): δ 1.04 (3H, t, $J = 7.2$ Hz), 1.49 (9H, s), 2.89–3.08 (6H, m), 3.44 (3H, s), 3.52–3.66 (4H, m), 3.72–3.82 (2H, m), 4.02–4.26 (2H, m), 5.26 (1H, br s), 6.82 (1H, d, $J = 8.0$ Hz), 6.83–7.03 (1H, m), 7.17–7.21 (1H, m), 7.26–7.74 (3H, m), 7.93 (1H, dd, $J = 7.6$, 2.0 Hz), 8.33 (1H, br s), 8.43 (1H, d, $J = 8.4$ Hz), 8.93 (1H, br s); MS (ESI) m/z $[\text{M} + \text{H}]^+$ 629.

5.1.10. *tert*-Butyl 4-{4-{4-[2-(ethylsulfamoyl)anilino]-1,3,5-triazin-2-yl}amino}-2-[2-(2-methoxyethoxy)ethoxy]phenyl}piperazine-1-carboxylate (**12b**)

Compound **12b** was prepared from **11b** and **3** in 44% yield using a

similar approach to that described for **12a**. $^1\text{H NMR}$ (CDCl_3): δ 1.04 (3H, t, $J = 7.6$ Hz), 1.49 (9H, s), 2.92–3.07 (6H, m), 3.37 (3H, s), 3.51–3.63 (6H, m), 3.69–3.71 (2H, m), 3.83–3.92 (2H, m), 4.07–4.23 (2H, m), 4.97 (1H, br s), 6.83–7.03 (2H, m), 7.17–7.21 (1H, m), 7.49–7.62 (1H, m), 7.93 (1H, dd, $J = 8.0$, 1.6 Hz), 8.38 (1H, br s), 8.45 (1H, d, $J = 8.0$ Hz), 8.93 (1H, br s); MS (ESI) m/z $[\text{M} + \text{H}]^+$ 673.

5.1.11. *N*-Ethyl-2-[(4-[3-(2-methoxyethoxy)-4-(4-methylpiperazin-1-yl)anilino]-1,3,5-triazin-2-yl)amino]benzene-1-sulfonamide (**13a**)

To a solution of **12a** (120 mg, 0.19 mmol) in CH_2Cl_2 (2 mL) was added TFA (1 mL). After stirring at room temperature for 1 h, the mixture was concentrated *in vacuo*. The residue was diluted with sat. NaHCO_3 aq, and extracted with $\text{CHCl}_3/\text{MeOH}$. The organic layer was dried over Na_2SO_4 and concentrated *in vacuo*. The residue was purified by column chromatography on silica gel ($\text{CHCl}_3/40\%$ CH_3NH_2 MeOH sol. = 100:0 to 60:1) to give the product (80 mg, 79%) as a gray solid. To a solution of the obtained intermediate (65 mg, 0.12 mmol) in CH_2Cl_2 (1.5 mL) was added 37% HCHO aq. (92 μL , 1.23 mmol). The mixture was stirred at room temperature for 1 h, and $\text{NaBH}(\text{OAc})_3$ (51 mg, 0.24 mmol) was added. After stirring at room temperature for 6 h, the mixture was neutralized with sat. NaHCO_3 aq, and extracted with CH_2Cl_2 . The organic layer was dried over Na_2SO_4 and concentrated *in vacuo*. The residue was purified by column chromatography on silica gel ($\text{CHCl}_3/\text{MeOH} = 40:1$ to 15:1) to give the product (35 mg, 53%) as a pale yellow solid. $^1\text{H NMR}$ (CDCl_3): δ 1.03 (3H, t, $J = 7.6$ Hz), 2.37 (3H, s), 2.52–2.74 (4H, m), 2.97 (2H, q, $J = 7.2$ Hz), 3.00–3.22 (4H, m), 3.44 (3H, s), 3.72–3.83 (2H, m), 4.02–4.20 (2H, m), 5.36 (1H, br s), 6.85–7.01 (2H, m), 7.16–7.20 (1H, m), 7.20–7.78 (3H, m), 7.93 (1H, dd, $J = 8.0$, 1.2 Hz), 8.33 (1H, br s), 8.44 (1H, d, $J = 8.4$ Hz), 8.93 (1H, br s); HRMS (ESI) m/z Calcd for $\text{C}_{25}\text{H}_{35}\text{N}_8\text{O}_4\text{S}$ $[\text{M} + \text{H}]^+$: 543.2496. Found: 543.2484.

5.1.12. *N*-Ethyl-2-[(4-{3-[2-(2-methoxyethoxy)ethoxy]-4-(4-methylpiperazin-1-yl)anilino]-1,3,5-triazin-2-yl)amino]benzene-1-sulfonamide (**13b**)

Compound **13b** was prepared from **12b** in 2 steps in 55% yield using a similar approach to that described for **13a**.

$^1\text{H NMR}$ (CDCl_3): δ 1.03 (3H, t, $J = 7.2$ Hz), 2.37 (3H, s), 2.52–2.72 (4H, m), 2.97 (2H, q, $J = 7.2$ Hz), 3.00–3.23 (4H, m), 3.36 (3H, s), 3.54–3.56 (2H, m), 3.69–3.72 (2H, m), 3.83–3.92 (2H, m), 4.04–4.21 (2H, m), 5.30 (1H, br s), 6.85–7.02 (2H, m), 7.16–7.20 (1H, m), 7.26–7.70 (3H, m), 7.93 (1H, dd, $J = 7.6$, 2.0 Hz), 8.35 (1H, br s), 8.43 (1H, d, $J = 8.4$ Hz), 8.93 (1H, br s); HRMS (ESI) m/z Calcd for $\text{C}_{27}\text{H}_{39}\text{N}_8\text{O}_5\text{S}$ $[\text{M} + \text{H}]^+$: 587.2759. Found: 587.2754.

5.1.13. 4-[3-(2-Chloro-5-nitrophenoxy)propyl]morpholine (**15a**)

To a solution of 2-(3-bromopropoxy)-1-chloro-4-nitrobenzene (**14**, 1.0 g, 3.40 mmol) in MeCN (20 mL) were added morpholine (355 μL , 4.07 mmol), K_2CO_3 (562 mg, 4.07 mmol) and KI (113 mg, 0.68 mmol). After stirring at 60 °C for 15 h, the mixture was diluted with H_2O and extracted with CHCl_3 . The organic layer was washed with brine, dried over MgSO_4 and concentrated *in vacuo*. The residue was purified by column chromatography on silica gel ($\text{CHCl}_3/\text{MeOH} = 100:0$ to 95:5) to give the product (646 mg, 63%) as a yellow solid. $^1\text{H NMR}$ (CDCl_3): δ 2.03–2.11 (2H, m), 2.43–2.52 (4H, m), 2.57 (2H, t, $J = 7.0$ Hz), 3.66–3.79 (4H, m), 4.21 (2H, t, $J = 6.3$ Hz), 7.39–7.63 (1H, m), 7.75–7.83 (2H, m); MS (ESI) m/z $[\text{M} + \text{H}]^+$ 301.

5.1.14. 4-{3-[2-(4-Methylpiperazin-1-yl)-5-nitrophenoxy]propyl}morpholine (**16a**)

To a solution of **15a** (400 mg, 1.33 mmol) in DMSO (3.3 mL) were added *N*-methyl-piperazine (293 μL , 2.66 mmol) and K_2CO_3 (368 mg, 2.66 mmol). After stirring at 150 °C overnight, the mixture was diluted with H_2O and extracted with CHCl_3 . The organic layer was dried over MgSO_4 and concentrated *in vacuo*. The residue was diluted with CHCl_3 . The organic layer was washed with H_2O and concentrated *in vacuo* to

give the product (200 mg, 41%). MS (ESI) m/z $[M+H]^+$ 365.

5.1.15. 4-[2-[2-(4-Methylpiperazin-1-yl)-5-nitrophenoxy]ethyl]morpholine (**16b**)

To a solution of 4-[2-(2-chloro-5-nitrophenoxy)ethyl]morpholine (**15b**, 731 mg, 2.42 mmol) in NMP (10 mL) were added *N*-methyl-piperazine (798 μ L, 7.25 mmol) and K_2CO_3 (1.00 g, 7.25 mmol). After stirring at 150 °C for 6 h, the mixture was diluted with H_2O and extracted with EtOAc. The organic layer was washed with brine, dried over Na_2SO_4 , and concentrated *in vacuo*. The residue was purified by column chromatography on amino functionalized silica gel (*n*-hexane/ $CHCl_3$ = 70:30 to 0:100) to give the product (465 mg, 55%) as a yellow oil. 1H NMR ($CDCl_3$): δ 2.35 (3H, s), 2.45–2.68 (8H, m), 2.80–2.90 (2H, m), 3.24–3.51 (4H, m), 3.53–3.81 (4H, m), 4.10–4.32 (2H, m), 6.88 (1H, d, J = 8.8 Hz), 7.71 (1H, d, J = 2.4 Hz), 7.86 (1H, dd, J = 8.8, 2.5 Hz); MS (ESI) m/z $[M+H]^+$ 351.

5.1.16. 1-Methyl-4-[2-[2-(4-methylpiperazin-1-yl)ethoxy]-4-nitrophenyl]piperazine (**16c**)

Compound **16c** was prepared from 1-[2-(2-chloro-5-nitrophenoxy)ethyl]-4-methylpiperazine (**15c**) in 43% yield using a similar approach to that described for **16b**. 1H NMR ($CDCl_3$): δ 2.30 (3H, s), 2.36 (3H, s), 2.39–2.72 (12H, m), 2.86 (2H, t, J = 5.6 Hz), 3.22–3.36 (4H, m), 4.19 (2H, t, J = 5.6 Hz), 6.87 (1H, d, J = 9.0 Hz), 7.70 (1H, d, J = 2.5 Hz), 7.85 (1H, dd, J = 8.9, 2.5 Hz); MS (ESI) m/z $[M+H]^+$ 364.

5.1.17. 4-(4-Methylpiperazin-1-yl)-3-[3-(morpholin-4-yl)propoxy]aniline (**17a**)

To a solution of **16a** (200 mg, 0.55 mmol) in EtOH (3.1 mL)/ H_2O (0.77 mL) were added $FeCl_3$ hexahydrate (45 mg, 0.16 mmol), activated carbon (46 mg) and hydrazine monohydrate (266 μ L, 5.49 mmol). After stirring at 100 °C for 18 h, the mixture was passed through a Celite pad and washed with EtOAc. The filtrate was dried over Na_2SO_4 and concentrated to give the product (170 mg, 93%) as a yellow solid. MS (ESI) m/z $[M+H]^+$ 335.

5.1.18. 4-(4-Methylpiperazin-1-yl)-3-[2-(morpholin-4-yl)ethoxy]aniline (**17b**)

Compound **17b** was prepared from **16b** in 100% yield using a similar approach to that described for **17a**. 1H NMR ($CDCl_3$): δ 2.35 (3H, s), 2.44–2.70 (8H, m), 2.77–2.88 (4H, m), 2.95–3.11 (4H, m), 3.66–3.77 (4H, m), 4.03–4.11 (2H, m), 6.18–6.32 (2H, m), 6.75–6.79 (1H, m); MS (ESI) m/z $[M+H]^+$ 321.

5.1.19. 4-(4-Methylpiperazin-1-yl)-3-[2-(4-methylpiperazin-1-yl)ethoxy]aniline (**17c**)

Compound **17c** was prepared from **16c** in 100% yield using a similar approach to that described for **17a** with the reaction temperature changed to 80 °C. 1H NMR ($CDCl_3$): δ 2.32–2.39 (3H, m), 2.47 (3H, s), 2.52–2.88 (14H, m), 3.03–3.19 (4H, m), 3.39–3.58 (2H, m), 4.04–4.11 (2H, m), 6.16–6.32 (2H, m), 6.74–6.80 (1H, m); MS (ESI) m/z $[M+H]^+$ 334.

5.1.20. *N*-Ethyl-2-[(4-{4-(4-methylpiperazin-1-yl)-3-[3-(morpholin-4-yl)propoxy]anilino}-1,3,5-triazin-2-yl)amino]benzene-1-sulfonamide (**18a**)

A mixture of **17a** (170 mg, 0.51 mmol) and AcOH (8.8 mL) was stirred at room temperature for 30 min before **3** (159 mg, 0.51 mmol) was added. After stirring at room temperature overnight, the mixture was concentrated *in vacuo*. The residue was diluted with sat. $NaHCO_3$ aq., and the mixture was extracted with $CHCl_3$. The organic layer was dried over Na_2SO_4 and concentrated *in vacuo*. The residue was purified by column chromatography on amino functionalized silica gel ($CHCl_3$ /MeOH = 100:0 to 90:10) to give the product (87 mg, 28%). 1H NMR ($DMSO-d_6$): δ 0.87–1.03 (3H, m), 1.77–1.96 (2H, m), 2.22 (3H, s), 2.28–2.50 (10H, m), 2.71–2.87 (2H, m), 2.87–3.03 (4H, m), 3.47–3.63 (4H, m), 3.77–4.10 (2H, m), 6.72–6.85 (1H, m), 6.95–7.15 (1H, m),

7.20–7.31 (1H, m), 7.34–7.51 (1H, m), 7.52–7.69 (1H, m), 7.81 (1H, dd, J = 7.9, 1.3 Hz), 7.87–8.05 (1H, m), 8.32–8.54 (2H, m), 9.02–9.28 (1H, m), 9.70–9.91 (1H, m); MS (ESI) m/z $[M+H]^+$ 612; HRMS (ESI) m/z Calcd for $C_{29}H_{42}N_9O_4S$ $[M+H]^+$: 612.3075. Found: 612.3076.

5.1.21. *N*-Ethyl-2-[(4-{4-(4-methylpiperazin-1-yl)-3-[2-(morpholin-4-yl)ethoxy]anilino}-1,3,5-triazin-2-yl)amino]benzene-1-sulfonamide (**18b**)

Compound **18b** was prepared from **17b** and **3** in 15% yield using a similar approach to that described for **18a**. 1H NMR ($DMSO-d_6$): δ 0.95 (3H, t, J = 7.2 Hz), 2.21 (3H, s), 2.36–2.53 (8H, m), 2.62–2.74 (2H, m), 2.83 (2H, q, J = 7.2 Hz), 2.90–3.03 (4H, m), 3.49–3.60 (4H, m), 3.88–4.06 (2H, m), 6.80 (1H, d, J = 8.6 Hz), 6.94–7.13 (1H, m), 7.19–7.29 (1H, m), 7.29–7.49 (1H, m), 7.50–7.69 (1H, m), 7.81 (1H, dd, J = 7.9, 1.5 Hz), 7.84–8.06 (1H, m), 8.28–8.70 (2H, m), 9.17 (1H, br s), 9.82 (1H, br s); MS (ESI) m/z $[M+H]^+$ 598; Anal. Calcd for $C_{28}H_{39}N_9O_4S$ ·0.2H₂O: C, 54.82; H, 6.96; N, 19.70; S, 5.01. Found: C, 54.78; H, 6.83; N, 19.73; S, 5.06.

5.1.22. *N*-Ethyl-2-[(4-{4-(4-methylpiperazin-1-yl)-3-[2-(4-methylpiperazin-1-yl)ethoxy]anilino}-1,3,5-triazin-2-yl)amino]benzene-1-sulfonamide tetrahydrochloride (**18c**)

The free form of **18c** was prepared from **17c** (157 mg, 0.47 mmol) and **3** (148 mg, 0.47 mmol) using a similar approach to that described for **18a**. To the free form of **18c** was added HCl (4.0 M 1,4-dioxane solution, 1.5 mL, 6.0 mmol). After stirring at room temperature overnight, the mixture was concentrated *in vacuo*. IPE/EtOAc was added to the residue, and the resulting precipitate was filtered and dried to give the product (112 mg, 31%) as a yellow solid. 1H NMR ($DMSO-d_6$): δ 0.95 (3H, t, J = 7.2 Hz), 2.76–2.92 (5H, m), 2.97–3.13 (2H, m), 3.18–3.33 (2H, m), 3.34–3.55 (4H, m), 3.56–3.89 (6H, m), 3.96–4.62 (9H, m), 6.88–7.01 (1H, m), 7.18–7.52 (3H, m), 7.61–7.73 (1H, m), 7.84 (1H, dd, J = 8.0, 1.2 Hz), 7.91–8.02 (1H, m), 8.16–8.60 (2H, m), 9.16–9.66 (1H, m), 9.77–10.41 (1H, m), 10.93 (1H, br s), 12.05 (1H, br s); MS (ESI) m/z $[M+H]^+$ 611; Anal. Calcd for $C_{29}H_{42}N_{10}O_3S$ ·4.3HCl·4.5H₂O: C, 41.04; H, 6.57; N, 16.51; S, 3.78; Cl, 17.96. Found: C, 41.20; H, 6.71; N, 16.31; S, 3.60; Cl, 17.86.

5.1.23. *tert*-Butyl {2-[(5-bromo-2-chloropyrimidin-4-yl)amino]benzene-1-sulfonyl}ethylcarbamate (**20**)

To a solution of *tert*-butyl (2-aminobenzene-1-sulfonyl)ethylcarbamate (**19**, 15.0 g, 49.9 mmol) in THF (120 mL) was added NaH (13.7 g, 59.9 mmol, 55% oil dispersion) in an ice-water bath. After stirring at room temperature for 1 h, 5-bromo-2,4-dichloropyrimidine was added to the mixture. After stirring at 50 °C for 12 h, the mixture was diluted with H_2O and extracted with EtOAc. The organic layer was washed with brine, dried over Na_2SO_4 and concentrated *in vacuo*. The residue was purified twice by column chromatography on silica gel (*n*-hexane/EtOAc = 95:5 to 50:50) to give the product (6.97 g, 28%) as a pale yellow solid. 1H NMR ($CDCl_3$): δ 1.30–1.40 (12H, m), 3.89 (2H, q, J = 7.0 Hz), 7.24–7.31 (1H, m), 7.61–7.69 (1H, m), 7.88 (1H, dd, J = 8.2, 1.6 Hz), 8.38 (1H, s), 8.42 (1H, dd, J = 8.4, 1.0 Hz), 9.59 (1H, s); MS (ESI) m/z $[M+H]^+$ 491.

5.1.24. 2-[(5-Bromo-2-[4-(1,4-dioxo-8-azaspiro[4.5]decan-8-yl)-3-methoxyanilino]pyrimidin-4-yl)amino]-*N*-ethylbenzene-1-sulfonamide (**22**)

To a solution of **20** (1.45 g, 2.95 mmol) in NMP/IPA (16 mL, 1:1) were added DIPEA (1.26 mL, 7.38 mmol) and 4-(1,4-dioxo-8-azaspiro[4.5]decan-8-yl)-3-methoxyaniline (**21**, 1.01 g, 3.84 mmol). After stirring at 150 °C under microwave irradiation for 14 h, the mixture was diluted with H_2O and extracted with EtOAc. The organic layer was washed with brine, dried over Na_2SO_4 and concentrated *in vacuo*. The residue was purified by column chromatography on silica gel (*n*-hexane/EtOAc = 90:10 to 0:100) to give the product (964 mg, 53%) as a colorless solid. 1H NMR ($CDCl_3$): δ 0.99–1.09 (3H, m), 1.85–1.99 (4H, m), 2.95–3.06 (2H, m), 3.06–3.17 (4H, m), 3.73 (3H, s), 3.97–4.05 (4H, m), 4.48 (1H, t, J = 6.0 Hz), 6.81–6.93 (2H, m), 6.95–7.11 (2H, m),

7.16–7.25 (1H, m), 7.48–7.56 (1H, m), 7.96 (1H, d, $J = 8.0$ Hz), 8.14–8.27 (1H, m), 8.41 (1H, d, $J = 8.4$ Hz), 8.97 (1H, s); MS (ESI) m/z $[M+H]^+$ 619, 621.

5.1.25. 2-((5-(3,5-Dimethoxyphenyl)-2-[3-methoxy-4-(4-oxopiperidin-1-yl)anilino]pyrimidin-4-yl)amino)-N-ethylbenzene-1-sulfonamide (**23**)

To a solution of **22** (188 mg, 0.30 mmol) in 1,4-dioxane (3.8 mL) were added Pd(PPh₃)₄ (35 mg, 0.030 mmol), 3,5-dimethoxyphenyl-bromic acid (110 mg, 0.61 mmol), and 2 M Na₂CO₃ aq. (379 μ L, 0.76 mmol) under an argon atmosphere. After stirring at 110 °C for 2 h, the mixture was diluted with EtOAc and passed through a Celite pad. The filtrate was concentrated *in vacuo*. The residue was purified by column chromatography on silica gel (*n*-hexane/EtOAc = 95:5 to 0:100) to give a pale yellow solid. To this product were added AcOH (4.0 mL, 48 mmol) and H₂O (8.0 mL). The mixture was stirred at 100 °C for 12 h and then concentrated *in vacuo*. The residue was neutralized with Na₂CO₃ aq. and extracted with CHCl₃. The organic layer was washed with brine, dried over Na₂SO₄ and concentrated *in vacuo*. The residue was purified by column chromatography on silica gel (CHCl₃/MeOH = 99:1 to 80:20) to give **23** (190 mg, 100%) as a brown solid. MS (ESI) m/z $[M+H]^+$ 633.

5.1.26. 2-([5-(3,5-Dimethoxyphenyl)-2-{3-methoxy-4-[4-(4-methylpiperazin-1-yl)piperidin-1-yl]anilino}pyrimidin-4-yl]amino)-N-ethylbenzene-1-sulfonamide (**24**)

To a solution of **23** (190 mg, 0.30 mmol) in CH₂Cl₂ (4.0 mL) was added *N*-methyl-piperazine (165 μ L, 1.5 mmol). After stirring at room temperature for 1 h, NaBH(OAc)₃ (80 mg, 0.38 mmol) was added. After stirring at room temperature for 1 h, NaBH(OAc)₃ (80 mg, 0.38 mmol) was added. After further stirring at room temperature for 12 h, the mixture was diluted with NaHCO₃ aq. and extracted with EtOAc. The organic layer was washed with brine, dried over Na₂SO₄ and concentrated *in vacuo*. The residue was purified by column chromatography on amino functionalized silica gel (EtOAc/MeOH = 100:0 to 80:20). IPE/EtOAc was added to the residue, and the resulting precipitate was filtered and dried to give the product (76 mg, 35%) as a colorless solid. ¹H NMR (DMSO-*d*₆): δ 0.91 (3H, t, $J = 7.2$ Hz), 1.45–1.60 (2H, m), 1.73–1.86 (2H, m), 2.15 (3H, s), 2.20–2.57 (11H, m), 2.68–2.78 (2H, m), 3.25–3.36 (2H, m), 3.51–3.65 (3H, m), 3.79 (6H, s), 6.51 (1H, dd, $J = 2.3, 2.2$ Hz), 6.66 (2H, d, $J = 2.4$ Hz), 6.72–6.80 (1H, m), 7.15–7.24 (2H, m), 7.33 (1H, d, $J = 2.2$ Hz), 7.48–7.57 (1H, m), 7.67 (1H, t, $J = 5.7$ Hz), 7.74 (1H, dd, $J = 7.8, 1.6$ Hz), 8.10 (1H, s), 8.42 (1H, d, $J = 8.2$ Hz), 8.78 (1H, s), 9.22 (1H, s); MS (ESI) m/z $[M+H]^+$ 717; HRMS (ESI) m/z Calcd for C₃₇H₄₉N₉O₅S $[M+H]^+$: 717.3541. Found: 717.3541.

5.1.27. Ethyl 4-[2-(ethylsulfamoyl)anilino]-2-(methylsulfanyl)pyrimidine-5-carboxylate (**27**)

To a solution of ethyl 4-chloro-2-(methylsulfanyl)pyrimidine-5-carboxylate (**25**, 4.65 g, 20 mmol) in toluene (58 mL) were added DIPEA (3.77 mL, 22 mmol) and 2-amino-*N*-ethylbenzene-1-sulfonamide (**26**, 4.01 g, 20 mmol). After stirring at 110 °C for 20 h, the solvent was replaced with NMP. After stirring at 130 °C for 6 h, the mixture was poured into H₂O. The resulting precipitate was filtered, washed with Et₂O and dried to give the product (5.61 g, 71%) as a colorless solid. ¹H NMR (CDCl₃): δ 1.02 (3H, t, $J = 7.2$ Hz), 1.41 (3H, t, $J = 7.1$ Hz), 2.46 (3H, s), 2.94–3.08 (2H, m), 4.44 (2H, q, $J = 7.0$ Hz), 4.89 (1H, br s), 7.23–7.32 (1H, m), 7.54–7.60 (1H, m), 8.03 (1H, d, $J = 7.8$ Hz), 8.24 (1H, d, $J = 8.4$ Hz), 8.84 (1H, s), 10.67 (1H, s); MS (ESI) m/z $[M+H]^+$ 397.

5.1.28. 4-[2-(Ethylsulfamoyl)anilino]-2-(methylsulfanyl)pyrimidine-5-carboxylic acid (**28**)

To a solution of **27** (1.98 g, 5.0 mmol) in MeOH/THF (20 mL, 1:1) was added 1 M NaOH aq. (20 mL, 20 mmol). After stirring at room temperature for 3 h, the mixture was neutralized with 1 M HCl aq. and

extracted with CHCl₃. The organic layer was washed with brine, dried over Na₂SO₄ and concentrated *in vacuo*. Et₂O was added to the residue, and the resulting precipitate was filtered and dried to give the product (1.50 g, 81%) as a colorless solid. ¹H NMR (DMSO-*d*₆): δ 0.84 (3H, t, $J = 7.2$ Hz), 2.36 (3H, s), 2.75–2.85 (2H, m), 7.31–7.39 (1H, m), 7.59–7.68 (2H, m), 7.85 (1H, dd, $J = 7.8, 1.2$ Hz), 8.02 (1H, d, $J = 8.2$ Hz), 8.74 (1H, s), 10.72 (1H, s), 13.54 (1H, br s); MS (ESI) m/z $[M+H]^+$ 369.

5.1.29. 4-[2-(Ethylsulfamoyl)anilino]-*N*-methoxy-*N*-methyl-2-(methylsulfanyl)pyrimidine-5-carboxamide (**29**)

To a solution of **28** (400 mg, 1.09 mmol) in DMF (8.00 mL) were added *N,O*-dimethylhydroxyamine hydrochloride (159 mg, 1.63 mmol), EDCI hydrochloride (312 mg, 1.63 mmol), HOBt (220 mg, 1.63 mmol) and Et₃N (303 μ L, 2.17 mmol). After stirring at room temperature for 12 h, the mixture was diluted with H₂O. The resulting precipitate was filtered and dried to give the product (429 mg, 96%) as a colorless solid. ¹H NMR (CDCl₃): δ 0.96 (3H, t, $J = 7.2$ Hz), 2.51 (3H, s), 2.87–3.01 (2H, m), 3.44 (3H, s), 3.66 (3H, s), 5.85–5.98 (1H, m), 7.19–7.31 (1H, m), 7.53–7.62 (1H, m), 8.04 (1H, d, $J = 8.0$ Hz), 8.39 (1H, d, $J = 8.2$ Hz), 8.58 (1H, s), 9.53 (1H, s); MS (ESI) m/z $[M+H]^+$ 412.

5.1.30. 2-([5-(3,5-Dimethoxybenzoyl)-2-(methylsulfanyl)pyrimidin-4-yl]amino)-*N*-ethylbenzene-1-sulfonamide (**30**)

To a solution of **29** (200 mg, 0.49 mmol) in THF (6.0 mL) was added 3,5-dimethoxyphenylmagnesium bromide (1.0 M THF solution, 1.7 mL, 1.7 mmol) at –78 °C. After stirring the mixture at –78 °C for 2 h and warming to room temperature, additional 3,5-dimethoxyphenylmagnesium bromide (1.0 M THF solution, 0.5 mL, 0.5 mmol) was added to the mixture at –78 °C. This sequence of steps was repeated twice with two further additions of 3,5-dimethoxyphenylmagnesium bromide (1.0 M THF solution, 1.0 mL, 1.0 mmol then 1.0 M THF solution, 1.9 mL, 1.9 mmol). After stirring at –78 °C for 2 h, the mixture was quenched with sat. NH₄Cl aq. and warmed to room temperature. The mixture was extracted with EtOAc. The organic layer was washed with brine, dried over Na₂SO₄ and concentrated *in vacuo*. The residue was purified by column chromatography on amino functionalized silica gel (CHCl₃) to give the product (150 mg, 63%) as a colorless solid. ¹H NMR (CDCl₃): δ 1.05 (3H, t, $J = 7.2$ Hz), 2.49 (3H, s), 3.00–3.11 (2H, m), 3.84 (6H, s), 5.17 (1H, t, $J = 5.9$ Hz), 6.68 (1H, dd, $J = 2.4, 2.2$ Hz), 6.83 (2H, d, $J = 2.4$ Hz), 7.26–7.34 (1H, m), 7.56–7.65 (1H, m), 8.06 (1H, dd, $J = 7.9, 1.5$ Hz), 8.31 (1H, dd, $J = 8.2, 1.0$ Hz), 8.58 (1H, s), 11.17 (1H, s); MS (ESI) m/z $[M+H]^+$ 489.

5.1.31. 2-([5-(3,5-Dimethoxybenzoyl)-2-{3-methoxy-4-[4-(4-methylpiperazin-1-yl)piperidin-1-yl]anilino}pyrimidin-4-yl]amino)-*N*-ethylbenzene-1-sulfonamide (**32**)

To a solution of **30** (150 mg, 0.31 mmol) in CH₂Cl₂ (4.0 mL) was added *m*-CPBA (75% wet, 78 mg, 0.34 mmol) in an ice-water bath. After stirring in an ice-water bath for 2 h, the mixture was quenched with NaHCO₃ aq. and extracted with EtOAc. The organic layer was washed with brine, dried over Na₂SO₄ and concentrated *in vacuo* to give 2-([5-(3,5-dimethoxybenzoyl)-2-(methanesulfinyl)pyrimidin-4-yl]amino)-*N*-ethylbenzene-1-sulfonamide (147 mg, 95%) as a brown solid, which was used in the next reaction without further purification. To a solution of 2-([5-(3,5-dimethoxybenzoyl)-2-(methanesulfinyl)pyrimidin-4-yl]amino)-*N*-ethylbenzene-1-sulfonamide (147 mg, 0.29 mmol) in IPA (4.0 mL) was added 3-methoxy-4-[4-(4-methylpiperazin-1-yl)piperidin-1-yl]aniline (**31**, 98 mg, 0.32 mmol). After stirring at 90 °C for 12 h, the mixture was diluted with NaHCO₃ aq. and extracted with EtOAc. The organic layer was washed with brine, dried over Na₂SO₄ and concentrated *in vacuo*. The residue was purified by column chromatography on amino functionalized silica gel (EtOAc/MeOH = 100:0 to 80:20) and then purified by column chromatography on silica gel (CHCl₃/MeOH = 100:0 to 80:20). EtOAc was added to the

residue, and the resulting precipitate was filtered and dried to give the product (89 mg, 41%) as a pale yellow solid. $^1\text{H NMR}$ (DMSO- d_6): δ 0.83–0.97 (3H, m), 1.44–1.58 (2H, m), 1.74–1.84 (2H, m), 2.15 (3H, s), 2.20–2.57 (11H, m), 2.79–2.90 (2H, m), 3.24–3.44 (5H, m), 3.82 (6H, s), 6.58–6.80 (4H, m), 7.02–7.16 (1H, m), 7.16–7.29 (1H, m), 7.32–7.43 (1H, m), 7.53–7.70 (2H, m), 7.87 (1H, dd, $J = 8.0, 1.6$ Hz), 7.95–8.09 (1H, m), 8.43 (1H, s), 9.96 (1H, br s), 11.35 (1H, br s); MS (ESI) m/z $[\text{M} + \text{H}]^+$ 745.

5.1.32. 2-[(5-[(3,5-Dimethoxyphenyl)(hydroxy)methyl]-2-{3-methoxy-4-[4-(4-methylpiperazin-1-yl)piperidin-1-yl]anilino}pyrimidin-4-yl)amino]-N-ethylbenzene-1-sulfonamide (33)

To a solution **32** (110 mg, 0.15 mmol) in THF/MeOH (6.0 mL, 2:1) was added NaBH_4 (10 mg, 0.26 mmol) in an ice-water bath. After stirring at room temperature for 1 h, NaBH_4 (10 mg, 0.26 mmol) was added to the mixture in an ice-water bath. After stirring at room temperature for 2 h, the mixture was concentrated *in vacuo*. The residue was purified by column chromatography on silica gel ($\text{CHCl}_3/\text{MeOH} = 100:0$ to $80:20$). IPE/EtOAc was added to the residue, and the resulting precipitate was filtered and dried to give the product (71 mg, 64%) as a pale yellow solid. $^1\text{H NMR}$ (DMSO- d_6): δ 0.91 (3H, t, $J = 7.1$ Hz), 1.43–1.59 (2H, m), 1.72–1.85 (2H, m), 2.16 (3H, s), 2.20–2.55 (11H, m), 2.78–2.90 (2H, m), 3.19–3.40 (2H, m), 3.46–3.55 (3H, m), 3.69 (6H, s), 5.69 (1H, d, $J = 3.7$ Hz), 6.33 (1H, d, $J = 3.9$ Hz), 6.37 (1H, dd, $J = 2.4, 2.2$ Hz), 6.64 (2H, d, $J = 2.4$ Hz), 6.69 (1H, d, $J = 8.6$ Hz), 7.13 (1H, d, $J = 8.0$ Hz), 7.16–7.24 (1H, m), 7.28 (1H, d, $J = 2.0$ Hz), 7.41 (1H, t, $J = 5.7$ Hz), 7.46–7.54 (1H, m), 7.80 (1H, dd, $J = 8.0, 1.6$ Hz), 7.92 (1H, s), 8.15 (1H, d, $J = 7.8$ Hz), 9.05 (1H, s), 9.18 (1H, s); MS (ESI) m/z $[\text{M} + \text{H}]^+$ 747.

5.1.33. 2-[(5-[(3,5-Dimethoxyphenyl)methyl]-2-{3-methoxy-4-[4-(4-methylpiperazin-1-yl)piperidin-1-yl]anilino}pyrimidin-4-yl)amino]-N-ethylbenzene-1-sulfonamide (34)

To a solution of **33** (53 mg, 71 μmol) in CH_2Cl_2 (2.0 mL) were added triethylsilane (113 μL , 0.71 mmol) and TFA (272 μL , 3.5 mmol) in an ice-water bath under an argon atmosphere. After stirring at room temperature for 18 h, additional triethylsilane (113 μL , 0.71 mmol) and TFA (1.0 mL, 13 mmol) were added to the mixture in an ice-water bath. After stirring at room temperature for 6 h, the mixture was concentrated *in vacuo*. The residue was purified by column chromatography on amino functionalized silica gel (EtOAc/MeOH = $100:0$ to $80:20$) and then purified by column chromatography on silica gel ($\text{CHCl}_3/\text{MeOH} = 100:0$ to $80:20$). IPE/EtOAc was added to the residue, and the resulting precipitate was filtered and dried to give the product (16 mg, 31%) as a colorless solid. $^1\text{H NMR}$ (DMSO- d_6): δ 0.91 (3H, t, $J = 7.2$ Hz), 1.45–1.60 (2H, m), 1.74–1.85 (2H, m), 2.18 (3H, s), 2.22–2.57 (11H, m), 2.69–2.81 (2H, m), 3.25–3.36 (2H, m), 3.60 (3H, s), 3.69 (6H, s), 3.78 (2H, s), 6.34 (1H, dd, $J = 2.2, 2.2$ Hz), 6.43 (2H, d, $J = 2.4$ Hz), 6.75 (1H, d, $J = 8.6$ Hz), 7.15–7.23 (2H, m), 7.28 (1H, d, $J = 2.0$ Hz), 7.49–7.57 (1H, m), 7.78 (1H, dd, $J = 7.8, 1.6$ Hz), 7.88 (1H, t, $J = 5.7$ Hz), 8.01 (1H, s), 8.56 (1H, d, $J = 8.6$ Hz), 8.80 (1H, s), 9.04 (1H, s); MS (ESI) m/z $[\text{M} + \text{H}]^+$ 731; HRMS (ESI) m/z Calcd for $\text{C}_{38}\text{H}_{51}\text{N}_8\text{O}_5\text{S}$ $[\text{M} + \text{H}]^+$: 731.3698. Found: 731.3688.

5.1.34. 2-[(5-Bromo-2-{3-methoxy-4-[4-(4-methylpiperazin-1-yl)piperidin-1-yl]anilino}pyrimidin-4-yl)amino]-N-ethylbenzene-1-sulfonamide (35a)

To a solution of **20** (1.0 g, 2.0 mmol) in IPA (10 mL) were added **31** (650 mg, 2.1 mmol) and methanesulfonic acid (0.40 mL, 6.1 mmol). After stirring at 130°C under microwave irradiation for 1 h, the mixture was quenched with NaHCO_3 aq. and extracted with EtOAc. The organic layer was washed with brine, dried over Na_2SO_4 and concentrated *in vacuo*. The residue was diluted with EtOAc and stirred under reflux conditions. After cooling to room temperature, the resulting precipitate was filtered and dried to give the product (1.0 g, 77%) as a colorless solid. $^1\text{H NMR}$ (CDCl_3): δ 1.04 (3H, t, $J = 7.2$ Hz), 1.73–1.96 (4H, m),

2.30 (3H, s), 2.34–2.75 (11H, m), 2.95–3.06 (2H, m), 3.43–3.55 (2H, m), 3.72 (3H, s), 4.44 (1H, t, $J = 6.1$ Hz), 6.80–6.88 (2H, m), 6.98 (1H, dd, $J = 8.5, 2.5$ Hz), 7.06 (1H, d, $J = 2.2$ Hz), 7.18–7.24 (1H, m), 7.47–7.55 (1H, m), 7.96 (1H, dd, $J = 7.9, 1.5$ Hz), 8.22 (1H, s), 8.39–8.44 (1H, m), 8.97 (1H, s); MS (ESI) m/z $[\text{M} - \text{H}]^-$ 657, 659.

5.1.35. 2-[(5-Bromo-2-[3-methoxy-4-(4-methylpiperazin-1-yl)anilino]pyrimidin-4-yl)amino]-N-ethylbenzene-1-sulfonamide (35b)

Compound **35b** was prepared from **20** and **2** in 73% yield using a similar approach to that described for **35a**. $^1\text{H NMR}$ (DMSO- d_6): δ 0.96 (3H, t, $J = 7.2$ Hz), 2.21 (3H, s), 2.37–2.53 (4H, m), 2.79–2.97 (6H, m), 3.59 (3H, s), 6.76 (1H, d, $J = 8.4$ Hz), 7.16 (1H, d, $J = 8.4$ Hz), 7.19–7.24 (1H, m), 7.24–7.32 (1H, m), 7.53–7.61 (1H, m), 7.82 (1H, dd, $J = 7.8, 1.6$ Hz), 7.85–7.93 (1H, m), 8.32 (1H, s), 8.39–8.52 (1H, m), 9.15 (1H, s), 9.31 (1H, s); MS (ESI) m/z $[\text{M} + \text{H}]^+$ 576, 578; HRMS (ESI) m/z Calcd for $\text{C}_{24}\text{H}_{31}\text{BrN}_7\text{O}_3\text{S}$ $[\text{M} + \text{H}]^+$: 576.1387. Found: 576.1381.

5.1.36. 2-[(5-[(3,5-Dimethoxyphenyl)ethynyl]-2-{3-methoxy-4-[4-(4-methylpiperazin-1-yl)piperidin-1-yl]anilino}pyrimidin-4-yl)amino]-N-ethylbenzene-1-sulfonamide (36)

To a solution of **35a** (900 mg, 1.4 mmol) in DMF (18 mL) were added $\text{Pd}(\text{PPh}_3)_4$ (315 mg, 0.27 mmol), 1-ethynyl-3,5-dimethoxybenzene (0.22 g, 1.4 mmol), and Et_3N (951 μL , 6.8 mmol) under an argon atmosphere. After stirring at 120°C for 0.5 h, additional 1-ethynyl-3,5-dimethoxybenzene (2.0 g, 12 mmol) in DMF (18 mL) was added dropwise to the mixture over 4 h. After stirring at 120°C for 2 h, the mixture was diluted with EtOAc and passed through a Celite pad. The filtrate was concentrated *in vacuo*. The residue was purified by column chromatography on silica gel ($\text{CHCl}_3/\text{MeOH} = 100:0$ to $80:20$) and then purified by column chromatography on amino functionalized silica gel (EtOAc/MeOH = $100:0$ to $80:20$). The residue was diluted with EtOAc and stirred under reflux conditions. After cooling to room temperature, the resulting precipitate was filtered and dried to give the product (771 mg, 76%) as a pale yellow solid. $^1\text{H NMR}$ (DMSO- d_6): δ 0.95 (3H, t, $J = 7.2$ Hz), 1.46–1.60 (2H, m), 1.75–1.85 (2H, m), 2.14 (3H, s), 2.20–2.56 (11H, m), 2.83–2.94 (2H, m), 3.26–3.38 (2H, m), 3.62 (3H, s), 3.77 (6H, s), 6.53 (1H, dd, $J = 2.4, 2.4$ Hz), 6.77–6.86 (3H, m), 7.16–7.30 (3H, m), 7.57 (1H, t, $J = 7.4$ Hz), 7.82 (1H, dd, $J = 8.0, 1.6$ Hz), 7.93–8.02 (1H, m), 8.40 (1H, s), 8.55–8.75 (1H, m), 9.52 (2H, br s); MS (ESI) m/z $[\text{M} + \text{H}]^+$ 741; Anal. Calcd for $\text{C}_{39}\text{H}_{48}\text{N}_8\text{O}_5\text{S}$. $0.3\text{EtOAc} \cdot 0.04\text{CHCl}_3$: C, 62.59; H, 6.58; N, 14.51; S, 4.15; Cl, 0.55. Found: C, 62.64; H, 6.61; N, 14.51; S, 4.08; Cl, 0.50.

5.1.37. 2-[(5-[2-(3,5-Dimethoxyphenyl)ethyl]-2-{3-methoxy-4-[4-(4-methylpiperazin-1-yl)piperidin-1-yl]anilino}pyrimidin-4-yl)amino]-N-ethylbenzene-1-sulfonamide (37)

To a solution of **36** (200 mg, 0.27 mmol) in THF/MeOH (8.0 mL, 1:1) was added 10% Pd/C (14 mg, 13 μmol) under an argon atmosphere. After stirring at room temperature under a hydrogen atmosphere (1.0 atm) for 6 h, the mixture was passed through a Celite pad. The filtrate was concentrated *in vacuo*. To the residue in THF/MeOH (8.0 mL, 1:1) was added 10% Pd/C (14 mg, 13 μmol) under an argon atmosphere. After stirring at room temperature under a hydrogen atmosphere (2.5 atm) for 4 h, the mixture was passed through a Celite pad. The filtrate was concentrated *in vacuo*. The residue was diluted with EtOAc and stirred under reflux conditions. After cooling to room temperature, the resulting precipitate was filtered and dried to give the product (102 mg, 51%) as a pale yellow solid. $^1\text{H NMR}$ (DMSO- d_6): δ 0.92–1.00 (3H, m), 1.45–1.60 (2H, m), 1.74–1.85 (2H, m), 2.14 (3H, s), 2.19–2.56 (11H, m), 2.69–2.90 (6H, m), 3.26–3.36 (2H, m), 3.61 (3H, s), 3.71 (6H, s), 6.30 (1H, dd, $J = 2.4, 2.2$ Hz), 6.50 (2H, d, $J = 2.4$ Hz), 6.76 (1H, d, $J = 8.8$ Hz), 7.15–7.24 (2H, m), 7.29 (1H, d, $J = 2.2$ Hz), 7.52–7.59 (1H, m), 7.80 (1H, dd, $J = 7.8, 1.6$ Hz), 7.95 (1H, t, $J = 5.5$ Hz), 8.02 (1H, s), 8.69 (1H, d, $J = 8.4$ Hz), 8.98 (1H, s), 9.01 (1H, s); MS (ESI) m/z $[\text{M} + \text{H}]^+$ 745; HRMS (ESI) m/z Calcd for

$C_{39}H_{53}N_8O_5S$ [M+H]⁺: 745.3854. Found: 745.3850; *Anal.* Calcd for $C_{39}H_{52}N_8O_5S \cdot 0.2EtOAc \cdot 1.7H_2O$: C, 60.3; H, 7.2; N, 14.1; S, 4.0. Found: C, 60.3; H, 7.0; N, 14.0; S, 3.8.

5.1.38. 2-[(2-Chloro-5-nitropyrimidin-4-yl)amino]-N-ethylbenzene-1-sulfonamide (**38**)

A mixture of **26** (510 mg, 2.6 mmol) and 2,4-dichloro-5-nitropyrimidine (530 mg, 2.6 mmol) in DMAc (5.0 mL) was stirred at room temperature for 3 h. The mixture was diluted with NaHCO₃ aq. and extracted with EtOAc. The organic layer was washed with brine, dried over MgSO₄ and concentrated *in vacuo*. The residue was purified by column chromatography on silica gel (*n*-hexane/EtOAc = 100:10 to 75:25) to give the product (720 mg, 77%) as a yellow solid. ¹H NMR (DMSO-*d*₆): δ 0.85 (3H, t, *J* = 7.2 Hz), 2.78 (2H, qd, *J* = 7.2, 5.8 Hz), 7.46–7.53 (1H, m), 7.71–7.80 (2H, m), 7.89–7.98 (2H, m), 9.31 (1H, s), 10.78 (1H, s); MS (ESI) *m/z* [M+H]⁺ 358.

5.1.39. N-Ethyl-2-[(2-{3-methoxy-4-[4-(4-methylpiperazin-1-yl)piperidin-1-yl]anilino}-5-nitropyrimidin-4-yl)amino]benzene-1-sulfonamide (**39a**)

Compound **39a** was prepared from **31** and **38** in 87% yield using a similar approach to that described for **18a**. ¹H NMR (DMSO-*d*₆): δ 0.77–0.88 (3H, m), 1.43–1.58 (2H, m), 1.74–1.84 (2H, m), 2.14 (3H, s), 2.18–2.57 (11H, m), 2.71–2.82 (2H, m), 3.26–3.35 (2H, m), 3.39 (3H, br s), 6.64 (1H, d, *J* = 8.2 Hz), 7.05 (1H, d, *J* = 8.0 Hz), 7.14 (1H, br s), 7.36–7.47 (1H, m), 7.53–7.66 (1H, m), 7.73–7.83 (1H, m), 7.88 (1H, d, *J* = 7.0 Hz), 7.94–8.07 (1H, m), 9.13 (1H, s), 10.37 (1H, br s), 10.82 (1H, br s); MS (ESI) *m/z* [M+H]⁺ 626.

5.1.40. 2-[(5-Amino-2-{3-methoxy-4-[4-(4-methylpiperazin-1-yl)piperidin-1-yl]anilino}pyrimidin-4-yl)amino]-N-ethylbenzene-1-sulfonamide (**39b**)

To a solution of **39a** (2.2 g, 3.5 mmol) in EtOH/THF (70 mL, 4:3) was added 10% Pd/C (50% wet, 1.6 g, 0.74 mmol) under an argon atmosphere. After stirring at room temperature under a hydrogen atmosphere (1.0 atm) for 6 h, the mixture was passed through a Celite pad. The filtrate was concentrated *in vacuo*. The residue was purified by column chromatography on silica gel (CHCl₃/MeOH/28% NH₃ aq. = 100:0:0 to 90:9:1) to give the product (2.1 g, 99%) as a brown solid. ¹H NMR (DMSO-*d*₆): δ 0.93 (3H, t, *J* = 7.2 Hz), 1.45–1.59 (2H, m), 1.73–1.85 (2H, m), 2.14 (3H, s), 2.17–2.54 (11H, m), 2.83 (2H, q, *J* = 7.0 Hz), 3.24–3.34 (2H, m), 3.62 (3H, s), 4.06 (2H, s), 6.74 (1H, d, *J* = 8.6 Hz), 7.12–7.22 (2H, m), 7.27 (1H, d, *J* = 2.4 Hz), 7.52–7.60 (1H, m), 7.75–7.83 (3H, m), 8.67 (1H, s), 8.71 (1H, d, *J* = 7.8 Hz), 9.01 (1H, br s); MS (ESI) *m/z* [M+H]⁺ 596.

5.1.41. N-(4-[2-(Ethylsulfamoyl)anilino]-2-{3-methoxy-4-[4-(4-methylpiperazin-1-yl)piperidin-1-yl]anilino}pyrimidin-5-yl)-3,5-dimethoxybenzamide (**40a**)

To a solution of **39b** (150 mg, 0.25 mmol) in THF (5.0 mL) were added DIPEA (50 μL, 0.29 mmol) and 3,5-dimethoxybenzoyl chloride (60 mg, 0.30 mmol). After stirring at room temperature for 1 h, the mixture was quenched with sat. NaHCO₃ aq. and extracted with CHCl₃/IPA (3:1). The organic layer was washed with brine, dried over Na₂SO₄ and concentrated *in vacuo*. The residue was purified by column chromatography on silica gel (CHCl₃/MeOH = 98:2 to 85:15). Et₂O was added to the residue, and the resulting precipitate was filtered and dried to give the product (93 mg, 49%) as a colorless solid. ¹H NMR (DMSO-*d*₆): δ 0.90 (3H, t, *J* = 7.2 Hz), 1.46–1.61 (2H, m), 1.75–1.86 (2H, m), 2.17 (3H, s), 2.22–2.59 (11H, m), 2.75–2.85 (2H, m), 3.26–3.38 (2H, m), 3.66 (3H, s), 3.83 (6H, s), 6.73 (1H, dd, *J* = 2.4, 2.2 Hz), 6.81 (1H, d, *J* = 8.6 Hz), 7.14–7.29 (5H, m), 7.52–7.63 (2H, m), 7.79 (1H, dd, *J* = 8.0, 1.6 Hz), 8.10 (1H, s), 8.78 (1H, d, *J* = 8.0 Hz), 9.20 (1H, s), 9.25 (1H, s), 9.88 (1H, s); MS (ESI) *m/z* [M+H]⁺ 760; *Anal.* Calcd for $C_{38}H_{49}N_9O_6S \cdot 0.05CHCl_3 \cdot 1.2H_2O$: C, 58.03; H, 6.59; N, 16.01; S, 4.07; Cl, 0.68. Found: C, 57.98; H, 6.50; N, 15.86; S, 4.03; Cl, 0.60.

5.1.42. N-(4-[2-(Ethylsulfamoyl)anilino]-2-{3-methoxy-4-[4-(4-methylpiperazin-1-yl)piperidin-1-yl]anilino}pyrimidin-5-yl)-2,5-dimethoxybenzamide (**40b**)

Compound **40b** was prepared from **39b** and 2,5-dimethoxybenzoic acid using a similar approach to that described for **40f**. MS (ESI) *m/z* [M+H]⁺ 760.

5.1.43. N-(4-[2-(Ethylsulfamoyl)anilino]-2-{3-methoxy-4-[4-(4-methylpiperazin-1-yl)piperidin-1-yl]anilino}pyrimidin-5-yl)-2,3-dimethoxybenzamide (**40c**)

Compound **40c** was prepared from **39b** and 2,3-dimethoxybenzoic acid using a similar approach to that described for **40f**. MS (ESI) *m/z* [M+H]⁺ 760.

5.1.44. N-(4-[2-(Ethylsulfamoyl)anilino]-2-{3-methoxy-4-[4-(4-methylpiperazin-1-yl)piperidin-1-yl]anilino}pyrimidin-5-yl)-3,5-dihydroxybenzamide (**40d**)

Compound **40d** was prepared from **39b** and 3,5-dihydroxybenzoic acid using a similar approach to that described for **40f**. MS (ESI) *m/z* [M+H]⁺ 732.

5.1.45. N-(4-[2-(Ethylsulfamoyl)anilino]-2-{3-methoxy-4-[4-(4-methylpiperazin-1-yl)piperidin-1-yl]anilino}pyrimidin-5-yl)-3,5-dimethylbenzamide (**40e**)

Compound **40e** was prepared from **39b** and 3,5-dimethylbenzoic acid using a similar approach to that described for **40f**. MS (ESI) *m/z* [M+H]⁺ 728.

5.1.46. N-(4-[2-(Ethylsulfamoyl)anilino]-2-{3-methoxy-4-[4-(4-methylpiperazin-1-yl)piperidin-1-yl]anilino}pyrimidin-5-yl)-4,6-dimethoxyppyrimidine-2-carboxamide (**40f**)

To a solution of **39b** (278 mg, 0.47 mmol) in DMF (5.0 mL) were added 4,6-dimethoxyppyrimidine-2-carboxylic acid (103 mg, 0.56 mmol), DIPEA (160 μL, 0.93 mmol) and HATU (236 mg, 0.62 mmol) in an ice-water bath. After stirring at room temperature overnight, the mixture was quenched with NaHCO₃ aq. and extracted with CHCl₃. The organic layer was washed with brine, dried over MgSO₄ and concentrated *in vacuo*. The residue was purified by column chromatography on silica gel (CHCl₃/MeOH/28% NH₃ aq. = 100:0:0 to 90:9:1). EtOAc/PE was added to the residue, and the resulting precipitate was filtered and dried. To the precipitate was added EtOH/EtOAc/MeCN, and the mixture was heated to 100 °C. After cooling to room temperature, the resulting precipitate was filtered and dried to give the product (96 mg, 27%) as a colorless solid. ¹H NMR (DMSO-*d*₆): δ 0.90 (3H, t, *J* = 7.2 Hz), 1.46–1.61 (2H, m), 1.74–1.86 (2H, m), 2.14 (3H, s), 2.20–2.58 (11H, m), 2.74–2.85 (2H, m), 3.25–3.39 (2H, m), 3.67 (3H, s), 4.03 (6H, s), 6.48 (1H, s), 6.82 (1H, d, *J* = 8.4 Hz), 7.16–7.29 (3H, m), 7.51–7.62 (2H, m), 7.77 (1H, dd, *J* = 7.9, 1.5 Hz), 8.13 (1H, s), 8.74–8.87 (1H, m), 9.14 (1H, br s), 9.27 (1H, s), 10.14 (1H, br s); MS (ESI) *m/z* [M+H]⁺ 762; *Anal.* Calcd for $C_{36}H_{47}N_{11}O_6S \cdot 1.7H_2O$: C, 54.56; H, 6.41; N, 19.44; S, 4.05. Found: C, 54.55; H, 6.38; N, 19.45; S, 4.02.

5.1.47. N-(4-[2-(Ethylsulfamoyl)anilino]-2-{3-methoxy-4-[4-(4-methylpiperazin-1-yl)piperidin-1-yl]anilino}pyrimidin-5-yl)-2,6-dimethoxyppyrimidine-4-carboxamide (**40g**)

Compound **40g** was prepared from **39b** and 2,6-dimethoxyppyrimidine-4-carboxylic acid using a similar approach to that described for **40f**. MS (ESI) *m/z* [M+H]⁺ 762.

5.2. Biology

5.2.1. In vitro kinase inhibitory assay

Inhibitory activity of compounds against FGFR1, 2, 3, and 4, and VEGFR2 were evaluated using an off-chip mobility shift assay.

FGFR1, 2, 3, and 4, and VEGFR2 kinase (Carna Bioscience, Kobe,

Japan) and test compounds were incubated for 30 or 120 min at room temperature (RT). After the incubation, substrate and adenosine triphosphate (ATP) at 75 $\mu\text{mol/L}$ for VEGFR2, FGFR2, and FGFR3, 125 $\mu\text{mol/L}$ for FGFR1, and 300 $\mu\text{mol/L}$ for FGFR4 were added and the reactions were incubated for 30 min at RT. The kinase reaction was stopped by the addition of termination buffer. The reaction mixtures were measured using an EZ Reader II (Perkin Elmer). Wells without ATP were measured as positive control (100% inhibition), and wells treated with DMSO were measured as a negative control (0% inhibition). The IC_{50} value of each experiment was calculated using Sigmoid-Emax non-linear regression analysis.

5.2.2. In vitro cell growth inhibitory assay

UM-UC-14 was purchased from ECACC (Salisbury, UK). The cell line was cultured according to instructions from the supplier. The cells were seeded in 384-well plates at 900 cells per well and incubated overnight. On the following day, the cells were exposed to compound **40a** for 5 days. Cell viability was measured using CellTiter-Glo (Promega, Madison, WI, USA). Data are presented as mean values from a single experiment performed in duplicate.

Funding

This research did not receive any specific grant from funding agencies in the public, commercial, or not-for-profit sectors.

Declaration of Competing Interest

This research is a collaboration between Astellas Pharma Inc. and Kotobuki Pharmaceutical Co., Ltd.

Acknowledgements

The authors thank Dr. Susumu Watanuki for his helpful support in the preparation of this manuscript. The authors thank Dr. Aya Kikuchi, Ms. Ayako Nakayama, Mr. Taisuke Nakazawa, and Dr. Masateru Iizuka for their contributions to the biological studies. The authors thank the staff of the Division of Analytical Science Laboratories and Astellas Research Technologies Co., Ltd. for conducting spectral measurements and elemental analysis.

References

- Ploeg M, Aben KKH, Kiemeny LA. The present and future burden of urinary bladder cancer in the world. *World J Urol.* 2009;27:289–293.
- Maase H, Sengelov L, Roberts JT, et al. Long-term survival results of a randomized trial comparing gemcitabine plus cisplatin, with methotrexate, vinblastine, doxorubicin, plus cisplatin in patients with bladder cancer. *J Clin Oncol.* 2005;23:4602–4608.
- Bischoff CJ, Clark PE. Bladder cancer. *Curr Opin Oncol.* 2009;21:272–277.
- Kim HS, Seo HK. Immune checkpoint inhibitors for urothelial carcinoma. *Investig Clin Urol.* 2018;59:285–296.
- Turner N, Grose R. Fibroblast growth factor signaling: from development to cancer. *Nat Rev Cancer.* 2010;10:116–129.
- Tomlinson DC, Baldo O, Harnden P, Knowles MA. FGFR3 protein expression and its relationship to mutation status and prognostic variables in bladder cancer. *J Pathol.* 2007;213:91–98.
- Guancial EA, Werner L, Bellmunt J, et al. FGFR3 expression in primary and metastatic urothelial carcinoma of the bladder. *Cancer Med.* 2014;3:835–844.
- Williams SV, Hurst CD, Knowles MA. Oncogenic FGFR3 gene fusions in bladder cancer. *Hum Mol Genet.* 2013;22:795–803.
- Nakanishi Y, Akiyama N, Tsukaguchi T, et al. Mechanism of oncogenic signal activation by the novel fusion kinase FGFR3-BAIAP2L1. *Mol Cancer Ther.* 2015;14:704–712.
- Cancer Genome Atlas Research Network. Comprehensive molecular characterization of urothelial bladder carcinoma. *Nature.* 2014;507:315–322.
- Goh YH, Yoo J, Noh JH, Kim C. Emerging targeted therapies in advanced bladder cancer. *Transl Cancer Res.* 2017;6:S666–S676.
- Taberero J, Bahleda R, Dienstmann R, et al. Phase I dose-escalation study of JNJ-42756493, an oral pan-fibroblast growth factor receptor inhibitor, in patients with advanced solid tumors. *J Clin Oncol.* 2015;33:3401–3408.
- Siefert-Radtke AO, Necchi A, Park SH, et al. First results from the primary analysis population of the phase 2 study of erdafitinib (ERDA; JNJ-42756493) in patients (pts) with metastatic or unresectable urothelial carcinoma (mUC) and FGFR alterations (FGFRalt). *ASCO Annual Meeting.* 2018;Abstract#:4503.
- Johnson & Johnson Home Page. BALVERSA™ (erdafitinib) receives U.S. FDA approval for the treatment of patients with locally advanced or metastatic urothelial carcinoma with certain FGFR genetic alterations. <https://www.jnj.com/balversa-erdafitinib-receives-u-s-fda-approval-for-the-treatment-of-patients-with-locally-advanced-or-metastatic-urothelial-carcinoma-with-certain-fgfr-genetic-alterations>.
- Squires M, Ward G, Saxty G, et al. Potent, selective inhibitors of fibroblast growth factor receptor define fibroblast growth factor dependence in preclinical cancer models. *Mol Cancer Ther.* 2011;10:1542–1552.
- Dieci MV, Arnedos M, Andre F, Soria JC. Fibroblast growth factor receptor inhibitors as a cancer treatment: From a biologic rationale to medical perspectives. *Cancer Discov.* 2013;3:264–279.
- Boss DS, Glen H, Beijnen JH, et al. A phase I study of E7080, a multitargeted tyrosine kinase inhibitor, in patients with advanced solid tumours. *Br J Cancer.* 2012;106:1598–1604.
- Renhowe PA, Pecchi S, Shafer CM, et al. Design, structure-activity relationships and in vivo characterization of 4-amino-3-benzimidazol-2-ylhydroquinolin-2-ones: A novel class of receptor tyrosine kinase inhibitors. *J Med Chem.* 2009;52:278–292.
- Trudel S, Li ZH, Wei E, et al. CHIR-258, a novel, multitargeted tyrosine kinase inhibitor for the potential treatment of t(4;14) multiple myeloma. *Blood.* 2005;105:2941–2948.
- Angevin E, Lin C, Pande AU, Lopez, J. A., Gschwend, J., Harzstark, A. L., Shi, M., Anak, O., Escudier, B. J.. A phase I/II study of dovitinib (TKI258), a FGFR and VEGFR inhibitor, in patients (pts) with advanced or metastatic renal cell cancer: Phase I results. *J Clin Oncol.* 2010;28:3057.
- Roodhart JM, Langenberg MH, Witteveen E, Voest EE. The molecular basis of class side effects due to treatment with inhibitors of the VEGF/VEGFR pathway. *Curr Clin Pharmacol.* 2008;3:132–143.
- Perera TPS, Jovcheva E, Mevellec L, et al. Discovery and pharmacological characterization of JNJ-42756493 (erdafitinib), a functionally selective small-molecule FGFR family inhibitor. *Mol Cancer Ther.* 2017;16:1010–1020.
- Guagnano V, Furet P, Spanka C, et al. Discovery of 3-(2,6-dichloro-3,5-dimethoxyphenyl)-1-(6-[4-(4-ethylpiperazin-1-yl)-phenylamino]-pyrimidin-4-yl)-1-methylurea (NVP-BGJ398), a potent and selective inhibitor of the fibroblast growth factor receptor family of receptor tyrosine kinase. *J Med Chem.* 2011;54:7066–7083.
- Brameld KA, Owens TD, Verner E, et al. Discovery of the irreversible covalent FGFR inhibitor 8-(3-(4-Acryloylpiperazin-1-yl)propyl)-6-(2,6-dichloro-3,5-dimethoxyphenyl)-2-(methylamino)pyrido[2,3-d]pyrimidin-7(8H)-one (PRN1371) for the treatment of solid tumors. *J Med Chem.* 2017;60:6516–6527.
- Mohammadi M, Froum S, Hamby JM, et al. Crystal structure of an angiogenesis inhibitor bound to the FGFR receptor tyrosine kinase domain. *EMBO J.* 1998;17:5896–5904.
- Kondoh Y, Iikubo K, Kuromitsu S, et al. *PCT Int Appl.* 2009;WO2009008371 (A1).
- Diels GSM, Ten Holte P, Freyne EJE, et al. *PCT Int Appl.* 2009;WO2009016132 (A1).
- Tomiyama T, Tomiyama Y, Yokota M, Muroga S. Jpn. Kokai Tokkyo Koho JP 2013-10712 A; 2013.
- Shimada I, Kurosawa K, Matsuya T, Iikubo K, Kondoh Y, Kamikawa A, Tomiyama H, Iwai Y. *PCT Int Appl.* 2019;WO2010128659 (A1).
- Nahm S, Weinreb SM. N-methoxy-N-methylamides as effective acylating agent. *Tetrahedron Lett.* 1981;22:3815–3818.
- Munikrishnappa CS, Puranik SB, Kumar GVS, Prasad YR. Part-1: Design, synthesis and biological evaluation of novel bromo-pyrimidine analogs as tyrosine kinase inhibitors. *Eur J Med Chem.* 2016;119:70–82.
- Feldman RI, Wu JM, Polokoff MA, et al. Novel small molecule inhibitors of 3-phosphoinositide-dependent kinase-1. *J Biol Chem.* 2005;280:19867–19874.
- McTiguea M, Murray BW, Chen JH, Denga YL, Solowiej J, Kania RS. Molecular conformations, interactions, and properties associated with drug efficiency and clinical performance among VEGFR TK inhibitors. *Proc Natl Acad Sci USA.* 2012;109:18281–18289.